

Abschlussbericht

zum Vorhaben

cLIFT – eine Hochdurchsatz-Synthesemethode für on-demand Molekülbibliotheken

Zuwendungsempfänger: Felix Löffler

Förderkennzeichen: 13XP5050A

Teil I: Kurzbericht

1. Ursprüngliche Aufgabenstellung sowie wissenschaftlicher und technischer Stand, an den angeknüpft wurde

Infektionskrankheiten sind eine ständige Belastung für die Gesundheit und die Wirtschaft. Weltweit können sie schwere Epidemien verursachen, die im Zusammenhang mit dem Klimawandel und Resistenzbildung das Potenzial haben, sich in große Pandemien zu entwickeln. Jüngste Forschungsergebnisse zeigen, dass die menschliche Antikörperantwort gegen eine Infektionskrankheit in verschiedenen Individuen und über Populationen hinweg ähnlich und konserviert ist. In anderen Worten: die Immunsysteme von verschiedenen Patienten zielen auf die gleichen Strukturen eines Krankheitserregers, um diesen zu bekämpfen. Doch für die meisten infektiösen Erreger sind diese Strukturen und die daran bindenden Antikörper unbekannt.

Um diese Strukturen zu identifizieren, müssen Bibliotheken mit Millionen verschiedener Moleküle analysiert werden, allerdings sind diese Screens bisher sehr teuer. Wir möchten daher eine Technologie entwickeln, mit der diese Molekülbibliotheken on-demand etwa 1.000-fach billiger und mit bisher unerreichter Flexibilität und Miniaturisierung herstellbar sind. Dies soll ein Syntheseroboter ermöglichen, dessen 2D-Laser-Scanning-System mit Laserpulsen definiert winzige Materialmengen aus einer Donorfolie präzise auf einen Syntheseträger überträgt (>100.000 Spots pro Glasobjektträger). Wenn nacheinander die Materialien aus verschiedenen Donorfolien übertragen werden, so kann ein nahezu beliebiges Muster von Molekülbausteinen erzeugt werden. Mittels chemischer Prozessierung und Wiederholung des Materialtransfers können in jedem Spot die Moleküle Lage für Lage synthetisiert werden. Wir möchten diese on-demand Molekülbibliotheken einsetzen um neue Biomarker und Impfstoffkandidaten zu finden. Falls es außerdem gelingt andere organische Moleküle im Arrayformat mit dieser Methode herzustellen, so eröffnet sich allein damit ein weites Forschungsfeld mit großen kommerziellen Chancen.

Im Zentrum des Forschungsprojekts stand die Technologie des Laser-induzierten Materialtransfers. Die chemischen Bausteine werden dabei zunächst zusammen mit dem bei Raumtemperatur festen Matrixmaterial in Lösung gebracht und auf "Donorträger" in einem dünnen Film aufgebracht (Spin Coating). Durch kombinatorischen Laser-induzierten Transfer ("combinatorial laser-induced forward transfer", cLIFT) wird das Material nun vom Donor auf definierte Positionen des Syntheseträgers aufgebracht. Mit dieser Technik konnten bereits kleinste Mengen an Synthesebausteinen mit höchster Präzision und sehr genau dosiert auf eine Oberfläche übertragen und in einem Proof-of-Principle am Beispiel einer Peptidbibliothek gezeigt werden.

Im Projekt sollten somit (1) die Optimierung der cLIFT-Methode für Peptidarrays vorangetrieben werden, (2) auf den cLIFT-Prozess basierende Protokolle zur Synthese organischer Substanzbibliotheken entwickelt werden und (3) verschiedene Anwendungen dieser Methoden für die Lebenswissenschaften verfolgt werden (*Infektionskrankheiten, Diagnostik*).

2. Ablauf des Vorhabens

Die wissenschaftlichen Ziele des Projekts wurden in fünf Arbeitspakete aufgeteilt:

- **AP 1:** Entwicklung und Design eines robusten Syntheseroboters (AP 1.1); Aufbau des Systems (AP 1.2); Charakterisierung und Optimierung des Matrix-Monomer-Gemischs im Hinblick auf ihre Eignung zur reproduzierbaren Herstellung von Materialspots (AP 1.3); weitere mechanische und technische Optimierung des Systems (AP 1.4).
- **AP 2:** Tieferes Verständnis des Übertrags mit numerischen Simulationen des Prozesses und Optimierung des Prozesses für höhere Spotdichten (AP 2.1); Optimierung der Herstellung des Donorträgerprozesses mittels Spin-Coating und Dip-Coating-Prozessen (AP 2.2); schnellere und automatisierte Herstellung der Donorträger (AP 2.2, AP 2.3); Automatisierung der Nasschemie (AP 2.4).
- **AP 3:** Einbau von posttranslational veränderten und synthetischen Bausteinen für die Synthese (AP 3): Dies eröffnet eine große Flexibilität in der Synthese um z.B. für AP 4 im Bereich der Infektionskrankheiten Proteine mit posttranslationalen Veränderungen darstellen zu können.
- **AP 4:** Proof-of-Principle der vollkombinatorischen Synthese mit cLIFT im Arrayformat und Auslesen

des Immunsystems mittels Proteom-weiten Mikroarrays; Biomarker identifizieren für Diagnostik- und Impfstoffentwicklung; Auslesen von Patientenseren (AP 4.1, 4.2, 4.3); Infektionskrankheiten: Flaviviren (z.B. Denguefieber, Zika), Malaria; Autoimmunerkrankungen, z.B. Multiple Sklerose.

- **AP 5:** Synthese von anderen Biomolekülen (Peptide, Glykane) mittels Lösungsmitteldampf.

Technische Arbeitsziele

- Herstellung von hochdichten Peptidarrays (≥ 10.000 Spots pro cm^2) für die Anwendung in den Lebenswissenschaften (AP 4).

Änderungen: Durch die Corona-Situation kam es in einigen Projektteilen zu deutlichen Verzögerungen (Laborschließungen, Lieferverzögerungen, keine Verfügbarkeit von Chemikalien und Standardlaborutensilien). Außerdem gab es auch Verzögerungen durch Mitarbeiter (Elternzeit, Suche und Einarbeitung neuer Mitarbeiter). Der Projektzeitplan hat sich insgesamt um 14 Monate verzögert. Eine zuwendungsneutrale Verlängerung wurde gewährt.

3. Wesentliche Ergebnisse sowie ggf. Zusammenarbeit mit anderen Forschungseinrichtungen

Entwicklung, Aufbau und Validierung der cLIFT-Maschine waren erfolgreich (AP 1). Die Auflösung (AP 2) konnte durch technische Optimierung und geschickte Ablagerung deutlich erhöht werden (bis zu 444,444 Spots pro cm^2). In AP 3 lag der Fokus Zwecks der Synthese von posttranslational veränderten Proteinfragmenten auf der Synthese von glykopeptidischen Mikroarrays. Somit konnten multivalente Bindungsinteraktionen präzise untersucht werden, einschließlich der Bindung von Lektinen an spezifische Zuckerreste. Diese Technologie ermöglichte eine detaillierte Analyse von Glykan-Protein-Wechselwirkungen. Darüber hinaus wurde die Synthese von Peptidoglykan-Fragmenten durchgeführt, was zu einer stärkeren Zusammenarbeit und gemeinsamen internationalen Förderung zur Weiterentwicklung dieser Technologie führte. In AP 4 wurde die cLIFT Technologie für die Herstellung hochdichter Peptidarrays zur Untersuchung von Virus- und Krankheitsantigenen eingesetzt. Diese und andere Technologien ermöglichten detaillierte Analysen der Antikörperantworten von Patienten auf das Ebola-Virus und den Zika-Virus sowie auf den Malaria Erreger. Dies lieferte wertvolle Einblicke in die Immunantwort und interessante Biomarker. Zudem wurden Antikörperantworten von Patienten und Impfprobanden bzgl. SARS-CoV-2 und MERS-CoV untersucht. Die Synthese von Oligosacchariden (AP5) wurde erstmals erfolgreich mittels Lösungsmittel- und Aktivator Dampf erzielt, was eine parallele Synthese auf Zellulosemembranen ermöglicht. Die Technologie wird nun für die Synthese auf Glaträgern optimiert. Durch die personellen Veränderungen in der Arbeitsgruppe die hauptsächlich der Coronalage geschuldet waren, gab es deutliche Verzögerungen (14 Monate) in den Anwendungen der cLIFT Methode bezüglich AP 3 – 5 (synthetische Aminosäurebausteine, Erforschung von Autoimmunerkrankungen, Glykansynthese mittels cLIFT). Es wurden viele Ergebnisse erfolgreich in hochrangigen wissenschaftlichen Journalen veröffentlicht. Die Entwicklung eines neuen Lasertransfer und Blitzsynthese Ansatzes erlaubt nun die Hochdurchsatz-Synthese von Fluoreszenzmolekülen aus einfachen Zuckermonomeren. Schließlich wurden alle zentralen Meilensteile am Projektende erfolgreich erreicht.

Viele dieser Ergebnisse wurden in Zusammenarbeiten mit diverse nationalen und internationalen Forschungseinrichtungen erhalten, wie z.B. international mit den Niederlanden (UMH Groningen; University of Amsterdam), UK (University of Oxford; University of Glasgow), China (Chinese University Hong Kong; ShanghaiTech University), Kanada (SFU Vancouver), USA (UC Denver; Uni Pittsburg), Brasilien (Fundação Oswaldo Cruz, Recife), Norwegen (Uni Oslo), als auch national (intern am MPIKG, Potsdam), KIT (Karlsruhe), UKE Hamburg, Uni Marburg, Uni Braunschweig, Uni Köln, TiHo Hannover, UK Frankfurt und FAU Erlangen.

Teil II: Eingehende Darstellung

1. Darstellung der Verwendung der Zuwendung sowie der erzielten Ergebnisse

WP 1 Development of a stable and reproducible cLIFT process

In WP 1, the goals were the development, design, and setup of a robust synthesis robot (WP 1.1 & 1.2), as well as its validation using 20 different amino acid building blocks (WP 1.3) and the mechanical and technical optimization of the combinatorial laser-induced forward transfer (cLIFT) process (WP 1.4). The concept of the cLIFT process is described in Fig. 1 (left).

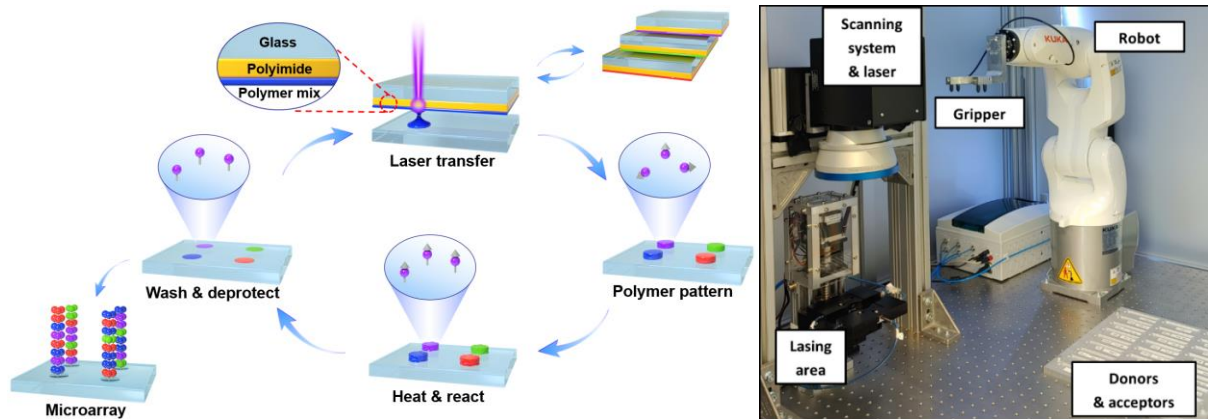


Figure 1. cLIFT method principle (left) and setup (right). A donor glass slide with self-adhesive polyimide foil, carrying an amino acid doped polymer matrix, is placed on top of a functionalized acceptor slide. Then, the laser transfers the polymer matrix, containing the amino acids, from the donor to the acceptor. Repeating this process with different building blocks allows for the creation of peptide microarrays. The automated setup with robot and laser system. [1]

The development, design, and setup of an automated cLIFT synthesizer that is robust and offers high precision was successful (Fig. 1 right). We developed a simple approach for laser calibration as well as a two-step alignment system. The laser system consists of a 300 mW TOPTICA iBeam smart laser with 405 nm wavelength, which is passed through an intelliSCAN III 10 laser scanning system (SCANLAB, Germany) equipped with an f-Theta-lens. This setup allows us to scan the focus ($\sim 60 \mu\text{m}$) of the laser beam in a plane and, thereby, reproducibly irradiate a surface at different positions to facilitate the laser-induced forward transfer.

To achieve high precision and reproducibility, we have built an automated setup with a KUKA robot to automatically pick and place the donor and acceptor slides (Fig. 1 right). A master computer controls the robot movement, mechanical alignment, laser activation, and timing for all actions. The RoboDK Python interface controls the robot, which transports the slides to the lasing area. First, an acceptor slide is transported/placed, held in place by vacuum, and pushed by pneumatic springs into the final processing location. Afterwards, a donor slide is placed on top of the acceptor slide and the laser receives a signal to initiate the process. Repeating these steps allows us to generate combinatorial patterns.

As a central milestone M1 of WP 1.3, all 20 standard amino acids were successfully transferred and reacted via cLIFT in an automated fashion with our setup (Fig. 1 right). After coupling in the oven and

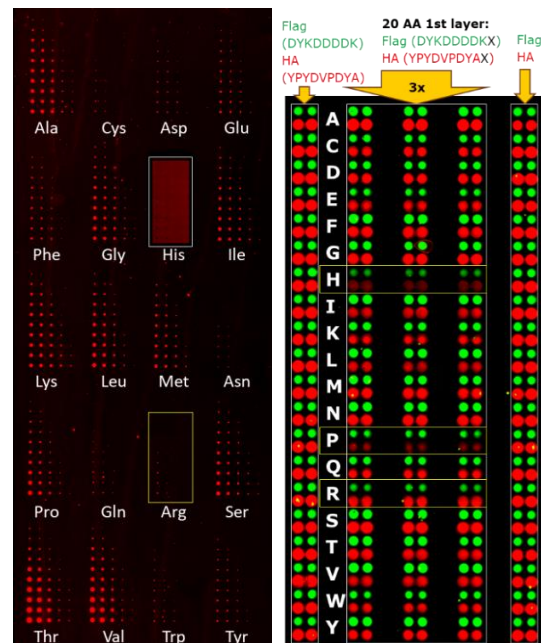


Figure 2. Validation of transfer of all 20 amino acids. (left) All 20 proteinogenic amino acids were transferred via cLIFT, coupled, and stained via biotin streptavidin labeling. Arg and His required additional validation. (right) Synthesis validation, using all 20 amino acids at the starting point of the standard peptides Flag and HA. His, Pro, and Arg were improved due to low antibody staining intensity. [1]

deprotection of side chains, all amino acids could be stained via biotin streptavidin labeling (Fig. 2 left). However, arginine (Arg) could only be validated via direct dye labeling, while histidine (His) only resulted in inverse staining (black spots, bright background). Difficulties of staining are known in literature, since different amino acids have different effects on dyes (quenching effect). We validated that the effect of histidine staining was not caused by degradation due to the laser transfer (stability measurements with HPLC of transferred amino acids). Also, the empty polymer alone (no amino acid inside) did not have any effect on surface staining. Next, we synthesized the control peptides Flag and HA with our setup (Fig. 2 right), either with the standard sequence, or with one additional (X) of the 20 amino acids at the bottom (synthesis starting at the C-terminus). While all peptides could be stained successfully, which indicates that the coupling was successful, we found three amino acids (His, Pro, Arg), which yield lower intensities upon staining. Therefore, we have developed a general optimization pipeline (Fig. 3), which can be applied once for each amino acid or any chemical building block to obtain a good parameter set for our specific setup and chemical reaction.

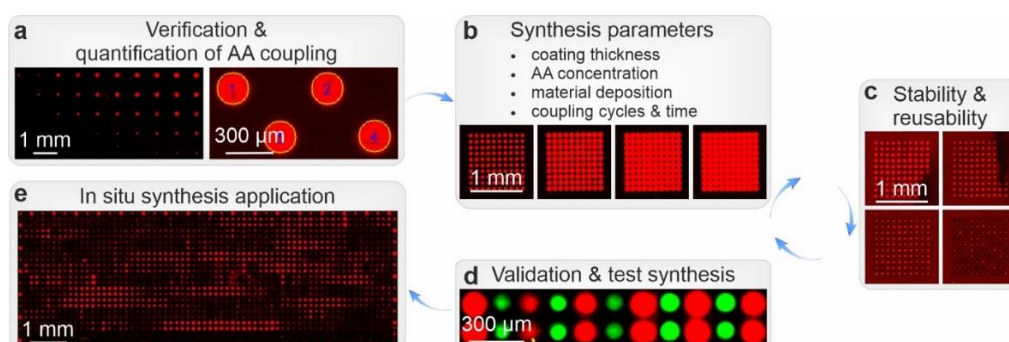


Figure 3. Optimization pipeline for the laser based in situ peptide microarray synthesis. (a) Verification and quantification of AA coupling is achieved by fluorescence labeling of amino groups and automated spot detection. (b) To obtain an optimal spot size and synthesis yield, parameters such as styrene-acrylic copolymer coating thickness, AA concentration, and AA dependent material deposition, as well as AA coupling cycles and time are investigated. (c) Afterwards, the stability and reusability of all AAs is assessed and (d) a validation synthesis is performed to determine the synthesis quality and yield of the found parameter sets. After several iterations, optimal parameters are obtained for all AAs, (e) which can be used for various applications (e.g., combinatorial peptide synthesis) [1].

After optimization, we increased the amount of amino acid building blocks inside the polymer for the critical amino acids, especially histidine (Fig. 4), and optimized the coupling cycles and times, to increase the coupling efficiency (Paris *et al.*, *Adv. Mater.* 2022).

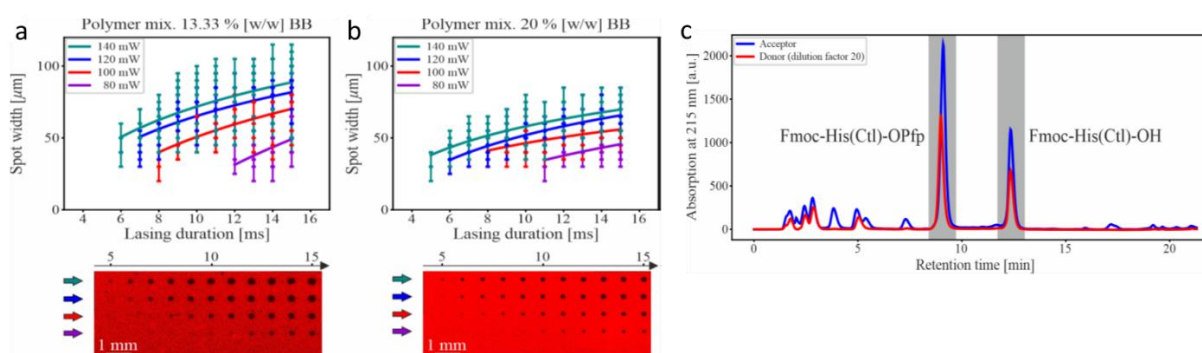


Figure 4. Validation of transfer of the (typically instable) histidine (H) building block. The amount of building block (% w/w) was increased to (a) 13.3 % and (b) 20 % w/w and tested with different laser parameters. As the only building block exception, histidine transfer resulted in inverse staining (black spots), upon staining the amino groups with a dye. Yet, we could validate the stability of histidine building block after laser transfer with HPLC analysis (c). The building block (red: before transfer) is not harmed by our laser transfer (blue: after transfer). [1]

For additional mechanical and technical optimizations (WP1.4) of the system, we have implemented a software step, where the user can intervene and easily continue the process after manual correction. We have synthesized validation arrays (Fig. 5, 150 μm spot-to-spot distance), containing the Flag and

HA epitopes, this time with all 20 amino acids in each layer. This allowed us to generate a substitution scan, replacing in the Flag and HA epitope sequentially one amino acid layer by all other 20 amino acids (Figure 5, highlighted in purple). We could successfully validate published specific antibody fingerprints, binding to the amino acid sequences of six amino acids DYKXXD (Flag) and DXPDYA (HA).

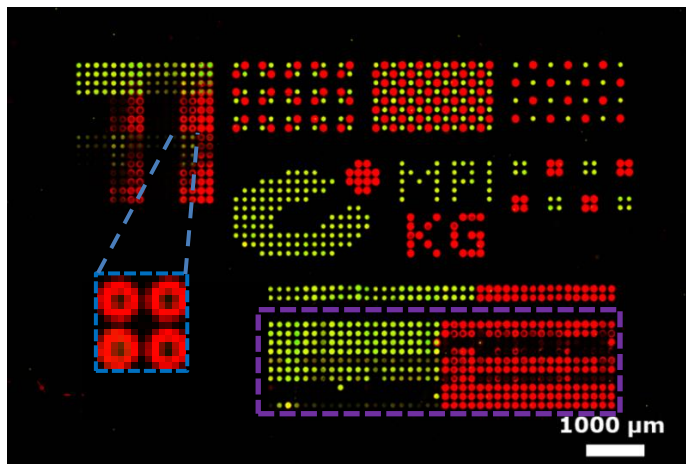


Figure 5. Validation synthesis of ~500 different Flag and HA control peptides (right), stained with anti-Flag (green) and anti-HA (red) antibodies. Full substitution scans with all 20 amino acids (highlighted in purple) reveal the specific antibody fingerprints, binding to the amino acid sequences DYKXXD (Flag) and DXPDYA (HA). [1]

production and we have successfully synthesized an Ebola proteome microarray and other microarrays (see WP4). The system is currently used for other projects. In a collaboration with the company Pepperprint GmbH in 2022, we performed a validation synthesis. Since 01/2023, Pepperprint is now employing a related machine setup for production of peptide arrays.

Major parts of WP1 with the setup and process have been published by us:

- [1] G. Paris, J. Heidepriem, A. Tsouka, Y. Liu, D. S. Mattes, S. Pinzón Martín, P. Dallabernardina, M. Mende, C. Lindner, R. Wawrzinek, C. Rademacher, P.H. Seeberger, F. Breitling, F.R. Bischoff, T. Wolf, **F.F. Loeffler**. Automated laser-transfer synthesis of high-density microarrays for infectious disease screening. *Advanced Materials*, **2022**, 34, 2200359

Notably, some spots feature a dark center with a red halo/circle (Figure 5, highlighted in blue). While the low central spot intensity is correct, according to literature, the halo is caused by slight differences in the spot sizes of differently transferred amino acid building blocks in different layers. This results in truncated peptides at the edges of some spots (circles), which still bind to the antibodies. Although this artifact can be omitted via software restriction, analyzing only a smaller central spot, we currently investigate the introduction of a pre patterning step before the synthesis with the amino acids aspartic acid or glutamic acid (Figure 6), which restricts the initial spot size to a minimum and reduces the halo effect.

The cLIFT system is now ready for

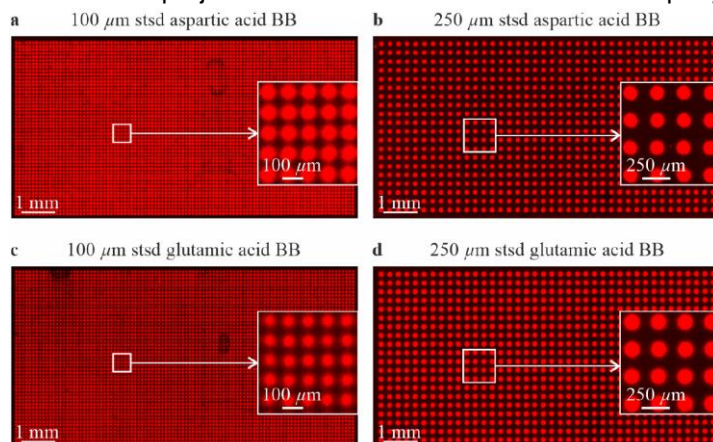


Figure 6. Acceptor slide pre patterning with aspartic acid (a, b) and glutamic acid (c, d) for 100 μm and 250 μm spot pitch (labeled with Biotin & CF633 streptavidin). [1]

WP 2 Increasing the spot density, process optimization

In WP 2, the main goals were to increase the spot density (WP 2.1), to optimize the production of the donor slides (WP 2.2), to make the reuse of donor slides possible (WP 2.3), and the automation of the wet chemistry processing (WP 2.4).

To better understand and further optimize our cLIFT process, we analyzed the laser transfer process in detail with a high-speed camera and developed a theoretical model (Fig. 7), which helped us to optimize the laser transfer. Derived from this model and the experimental data, the transfer can be explained as a short contact process, similar to the type writing process. The data was published:

- [2] G. Paris, A. Klinkusch, J. Heidepriem, A. Tsouka, J. Zhang, M. Mende, D. Mattes, D. Mager, H. Riegler, S. Eickelmann, **F. F. Loeffler**. Laser-induced forward transfer of soft material nanolayers with millisecond pulses shows contact-based material deposition. *Appl. Surf. Sci.*, **2020**, 508, 144973

- [3] G. Paris, D. Bierbaum, M. Paris, D. Mager, **F.F. Loeffler***. Development and Experimental Assessment of a Model for the Material Deposition by Laser-Induced Forward Transfer. *Applied Sciences*, **2022**, 12, 1361

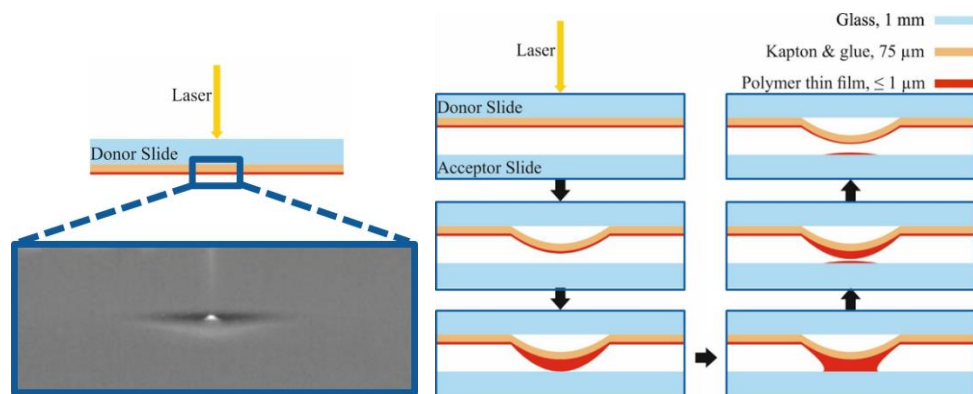


Figure 7. Analysis of the transfer process. (left) During laser irradiation, a high-speed camera captures the surface evolution (blister formation) of the donor slide with 39k fps. (right) According to this data, we derived a theoretical model, which explains the transfer as a short contact, similar to a type writing process. [2]

To further optimize our process and increase the spot density, we strived to understand, which temperatures are reached on the donor surface *via* laser heating. Typically, short-lived micro-sized thermal gradients are challenging to measure. In our process, it is important to know the exact temperature profile to assure the stability of sensitive building blocks. Many theoretical models try to describe the occurring temperatures, but still lack in profound experimental data. Therefore, we developed a facile approach [4], which allows to measure confined temperature gradients with millisecond and micrometer precision. By casting a thin alkane film onto a donor slide, it is possible to reconstruct local temperature gradients by imaging the phase behavior and morphology of the alkane film with a simple optical microscope setup (Figure 8a-c). Alkanes are inert and their melting and boiling temperatures depend on the chain length. This allows to measure temperatures between 37 and 522 °C on any surface (Figure 8d). Furthermore, after thorough characterization of laser-induced temperature gradients, this approach can be used to measure the phase transition behavior of complex thin film polymer mixtures.

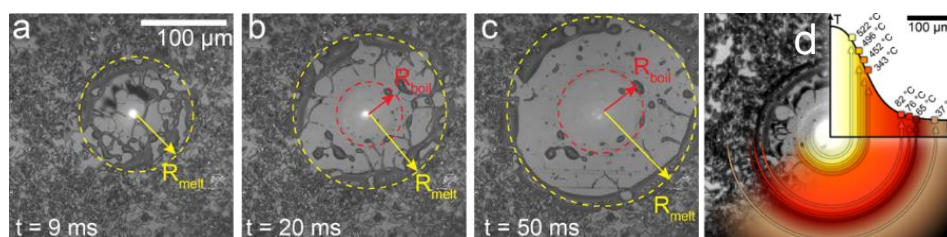


Figure 8. Time evolution of an alkane film on a donor slide, melting during laser irradiation: (a) Initial melting due to laser irradiation, rupture of film and ring formation (b). Evaporation of tiny residual alkane droplets (c), revealing the boiling of the alkane layer in a ring. (d) Temperature gradient, derived from the measurements. [4]

This concept has been published:

- [4] S. Eickelmann, S. Ronneberger, J. Zhang, G. Paris, **F.F. Loeffler**. Alkanes as intelligent surface thermometers: a facile approach to characterize short-lived temperature gradients on the micrometer scale. *Advanced Materials Interfaces*, **2021**, 8, 2001626

Increasing the spot density (WP 2.1)

The previous technological analyses, together with optimized donor slides (see WP 2.2), enabled us to increase the printed spot density (WP 2.1) and achieve the central milestone M2 of WP2, achieving a spot-to-spot distance of $\leq 100 \mu\text{m}$. This allows for 10 000 spots per cm^2 , resulting in up to 200 000 spots per slide. To validate the peptide synthesis quality at this resolution, we have performed the synthesis of up to 20-mer peptides, containing the Flag epitope. Since the binding of the anti-Flag antibody is only mildly influenced by the preceding amino acids of the epitope, we chose this peptide. First, we have attached a pre patterning amino acid (Asp = D, Glu = E) on the surface, followed by all 20 amino acids

and a subsequent Flag epitope (Figure 9 left). The pre patterning makes the spot intensity and the spot size (not shown) more stable. Since the amount of transferred material is much lower for the 100 μm pitch synthesis, the general spot intensity is only about 40 % of the 250 μm synthesis. However, this should be sufficient for a readout of antibody binding. In addition, we have synthesized Flag epitopes with a preceding glycine-serin spacer up to 20-mer peptides, to compare the coupling yield (Figure 9 right). We achieve a high yield for the 250 μm peptide synthesis.

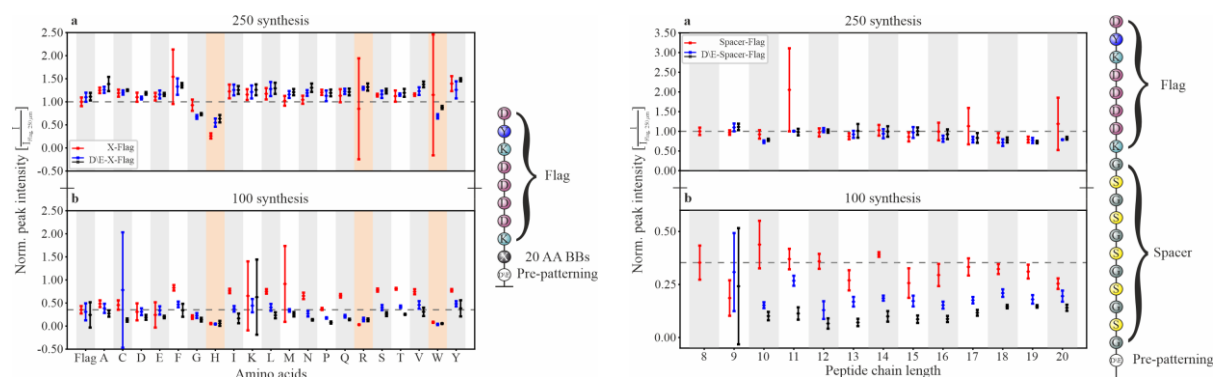


Figure 9. Synthesis quality using the Flag epitope. (left) Spot peak staining intensity, depending on the amino acid coupling yield, with and without pre patterning (D, E). (right) Spot peak intensity for peptides with increasing length (8-mer to 20-mer), introducing an increasing glycine-serine spacer [1].

In addition, to reach even higher spot densities, we hypothesized that the resolution is mainly related to the absorber foil on the donor slides, which consists of a 25 μm thick polyimide foil. In a new approach, we propose to replace polyimide by a robust hematite ($\alpha\text{-Fe}_2\text{O}_3$) nanolayer (< 500 nm thin) as the absorber for high-resolution LIFT. The hematite nanolayer can be obtained by a facile spin coating of iron precursor and oven annealing process and shows to be stable on the acceptor surface. Since the inorganic hematite is much thinner and more stable than polyimide, it shows less heat conduction and smaller spots. For parallel amino acid coupling reactions, our hematite donor enables five times higher patterning resolution (> 111,000 spots/cm²) with more efficient scanning (2 vs. 6 ms per spot) compared with the standard polyimide donor (Fig. 10).

Since this hematite nanolayer is wettable by both aqueous and organic solvents, the new donor significantly increases the scope of polymers for the LIFT process. This opens up many new research fields to this technology. Due to the now much larger polymer scope (we can now also transfer water-soluble polymers), we could explore the possibility to run so far to us inaccessible types of reactions inside polymer nanoreactors, such as copper catalyzed click chemistry, suggesting the potential of LIFT for both chemical deposition and in-situ

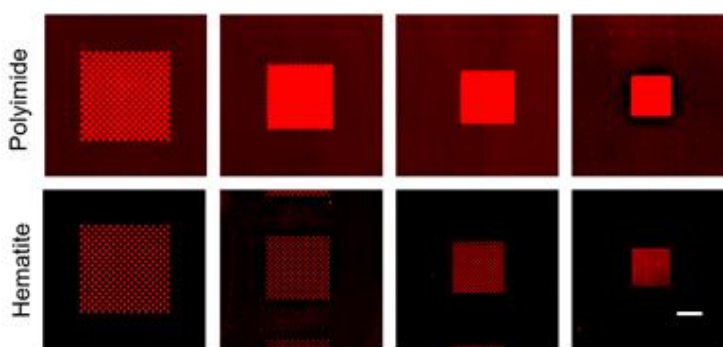


Figure 10. New hematite donor slides in LIFT. Amide bond formation in a chess-board pattern (25 x 25 theoretical spots), achieved for different pitches/spot densities, from left to right: 70 μm , 50 μm , 40 μm , 30 μm . Hematite allows for much higher densities without merging/overlapping of spots. [5]

synthesis. Furthermore, the high temperature stability of hematite makes it ideal for controlled material synthesis, opening many new research fields.

The process for high spot densities and new chemical reactions and the transfer of different polymers have been published:

- [5] J. Zhang, Y. Liu, S. Ronneberger, N.V. Tarakina, N. Merbouh, **F.F. Loeffler**. Nanolayer laser absorber for femtoliter chemistry in polymer reactors. *Advanced Materials*, **2022**, 2108493
- [6] S. Eickelmann, S. Moon, Y. Liu, B. Bitterer, S. Ronneberger, D. Bierbaum, F. Breitling, **F.F. Loeffler**. Assessing Polymer-Surface Adhesion with a Polymer Collection. *Langmuir*, **2022**, 38, 2220–2226

Finally, by exploiting this new hematite donor, we developed an even higher precision for printing in

another recent work [7]. We showed that our LIFT process enables a material position printing precision of $<1\ \mu\text{m}$, which is much higher than standard inkjet printers. Without adjusting the polymer matrix or printing process, our technique enables printing on multiple substrates, such as paper, glass, aluminum, or plastic foil (Figure 11).

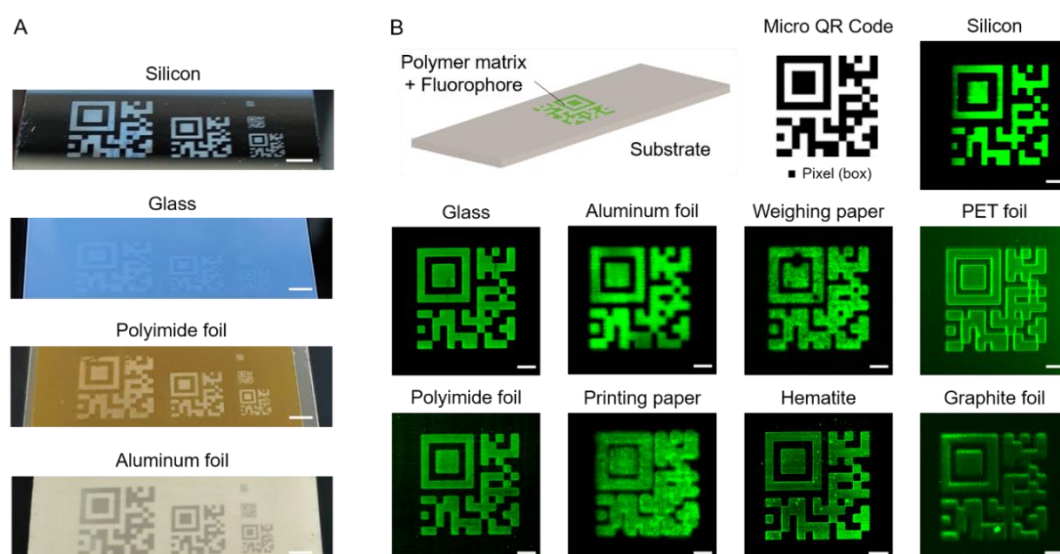


Figure 11. (A) Printing results on substrate collection. Scale bar 2 mm. (B) Fluorescence scans of printed fluorophore doped polymer micro QR codes on different substrates. Scale bars 500 μm [7].

Since the printing process is solvent-free, it is much less prone to contamination or misprinting by nozzle clogging. By exploiting these new high-resolution printing capabilities, we could introduce a sub-position writing approach, which we applied for fluorescent surface labeling (Fig. 12).

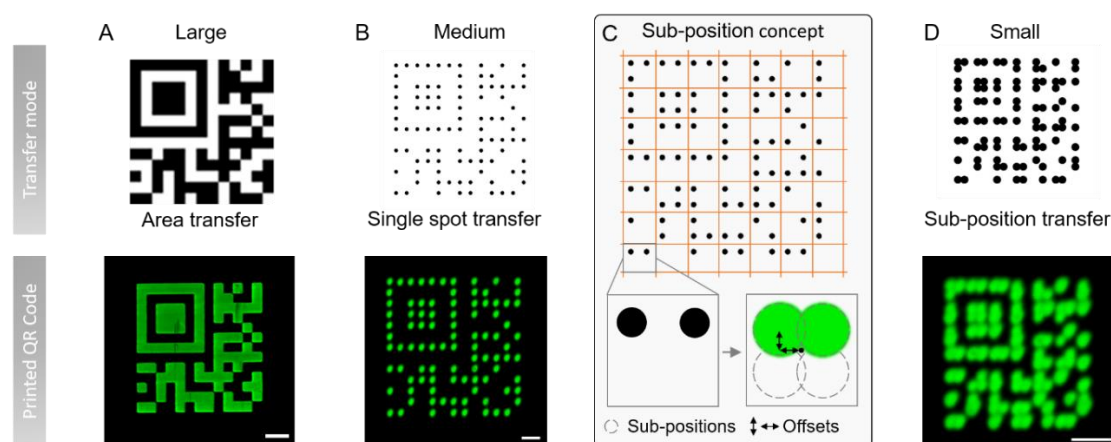


Figure 12. Different printing modes of the same QR code, reaching different pattern sizes on standard microscope glass. (A) Large-scale printing by area transfer mode (scale bar 500 μm). (B) Medium size printing with single polymer spot transfers (scale bar 100 μm). (C, D) By introducing the sub-position concept, an even higher resolution can be achieved (scale bar 50 μm) [7].

Each position is composed of multiple overlapping sub-spots, which can now be deconvoluted by a machine learning algorithm to read the data. This allowed us to create patterns with much higher data density than recently reported inkjet-printed binary information storage, with only two (instead of seven) fluorophores and a simple fluorescence scanner (without high resolution confocal microscopy). This enables high-resolution fluorescent labels with comparable spot-to-spot distance of down to 15 μm (444,444 spots/cm²) and rapid machine learning-supported readout based on low-resolution fluorescence imaging. In the future, this could significantly improve the density of synthesized microarrays. These findings have been published:

[7] S. Ronneberger, J. Zhang, Y. Liu, **F.F. Loeffler***. Solid ink laser patterning for high-resolution information labels with supervised learning readout. *Advanced Functional Materials*, **2023**, 33, 2210116

Optimizing donor slide production & reuse (WP 2.2 & 2.3)

For the optimization of donor slide production (WP 2.2) and the reuse of donor slides (WP 2.3), we first developed a homebuilt laminator, which was refined by the MPICI workshop, to quickly and semi-automatically coat glass slides with the self-adhesive polyimide laser absorber film (Fig. 13).



Figure 13. Homebuilt laminator for semi-automatic donor slide fabrication, for coating glass slides with self-adhesive polyimide tape.

Next, we thoroughly investigated the spin coating protocol (Fig. 14 left), to find optimum parameters for coating and peptide synthesis. To reduce the amount of required material, we investigated optimal lasing parameters together with the step-wise reduction of materials and solvents, as well as the reuse of donor slides. We transferred, coupled, and stained amino acid derivatives on commercially available Pepperprint slides and measured the spot width (Fig. 14 right). While some amino acid contents could be reduced, others had to be increased to achieve high coupling yields.

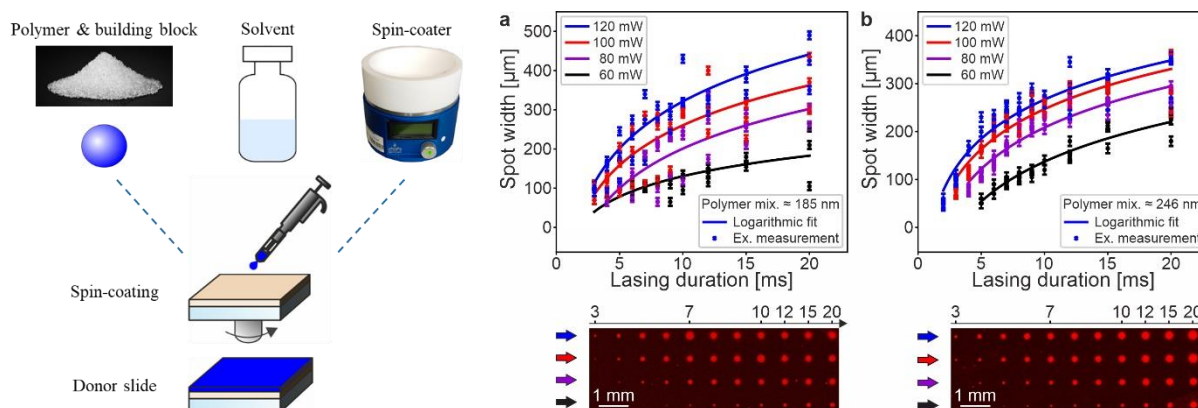


Figure 14. (left) Investigation of spin coating protocol. (right) Different lasing parameters were tested for all 20 amino acids for optimal transfer results. Example data for lasing power and duration vs. spot width for varying polymer coating thicknesses ((a) 185 nm, (b) 246 nm). [1]

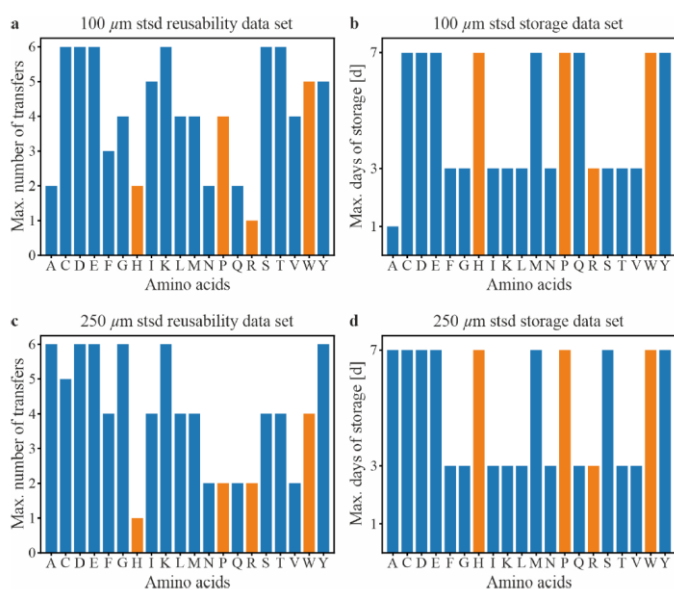


Figure 15. The reusability and storage (in days) of donor slides for a pitch of 100 μm (a, b) and 250 μm (c, d). Four building blocks, which were subsequently optimized, are highlighted in orange. [1]

For the 250 μm pitch, all slides can be used for at least 3 days and at least twice (except for histidine). For the 100 μm spot pitch, the picture slightly changes.

We first developed a protocol to correlate parameters, such as donor polymer coating thickness, polymer type, and amino acid concentration vs. transferred spot width. For sensitive amino acid building blocks, such as histidine, additional stability analyses with mass spectrometry were performed. An automated software for fluorescence readout was developed. All 20 amino acid building blocks were analyzed and optimized (optimization protocol shown in Fig. 3). Data can be found in the PhD thesis of Dr. Grigori Paris (2021, TU Berlin).

For WP2.3, the reuse of donor slides, we have derived a set of parameters for each amino acid building block type (Fig. 15). The higher the spot density, the less a donor slide can be reused, since the quality of transfer suffers from the reuse.

Automation of wet chemistry (WP 2.4)

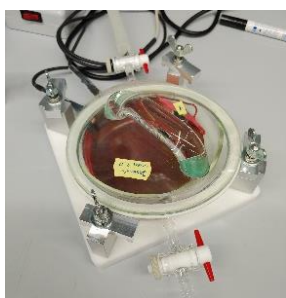


Figure 16. Electrically powered coupling oven for rapid and homogeneous heating under inert conditions to 95 °C, built by the MPICI workshop.

Due to personnel changes and the Corona situation, we were not able to automate the wet chemistry process (WP 2.4). The postdoctoral researcher planned for this investigation, unfortunately left the research group for an industry position. However, a collaboration with the company Pepperprint was started, since they already have a functioning automated wet chemistry setup. The usefulness of such a device is only given, if many microarrays are produced in parallel, which is rarely the case for us.

In addition, we developed an electrically powered coupling oven (Fig. 16) for rapid and homogeneous heating under inert conditions to 95 °C, built by the MPICI workshop. This allows for the coupling reaction of the amino acid building blocks to the functionalized array surface within 10 minutes, which has significantly reduced the required processing time by a factor of nine.

WP 3 Posttranslationally modified and non-physiological amino acids

In WP 3, the goal was to incorporate posttranslationally modified amino acids into the cLIFT process (WP 3.1), as well as synthetic building blocks (WP 3.2).

Therefore, we explored our laser-based cLIFT technology for on-chip glycopeptide synthesis. We can quickly synthesize different peptides directly on-chip as multivalent scaffolds. Together with click chemistry, we can attach different azido-sugars to the scaffolds with defined spacing and density. First, we synthesized arrays of different synthetic peptide sequences, containing various numbers of the alkyne-functionalized amino acid l-propargylglycine (Fig. 17). Subsequently, we used click chemistry to attach azido-functionalized sugars to these distinct positions on the peptide backbone (from solution, not via cLIFT). We studied the interactions of the fluorescently labelled lectins concanavalin A (ConA) and human langerin (in collaboration with Dr. Alvaro Mallagary, Uni Lübeck; Dr. Rademacher, Dr. Delbianco, MPICI). We found a significant spacing-, density-, and ligand-dependency (Fig. 18).

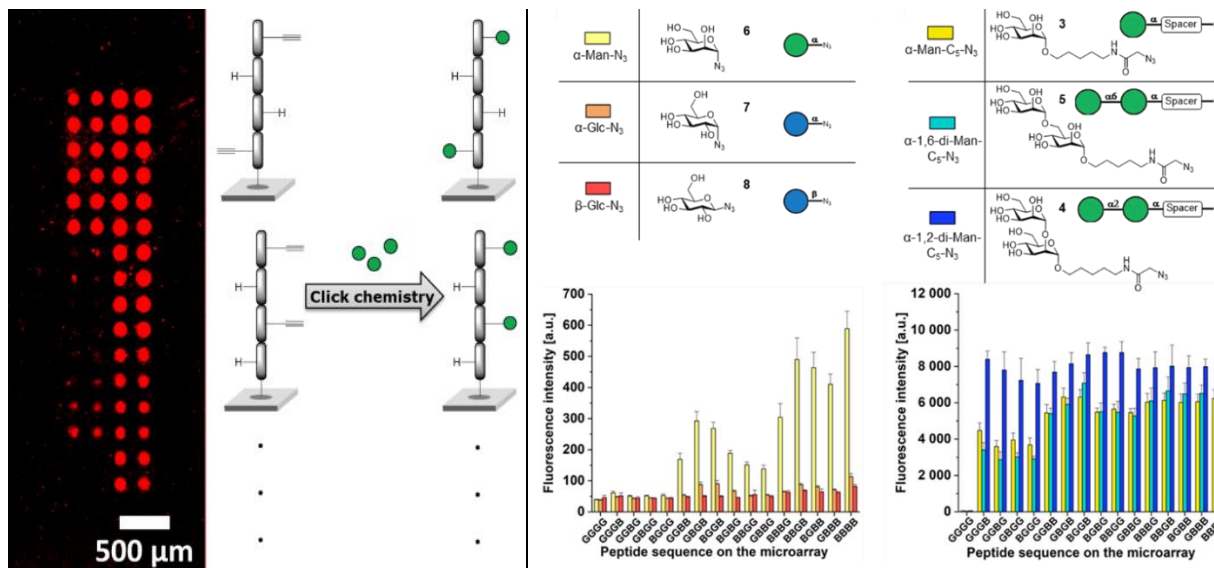


Figure 17. Glycopeptide array stained with ConA. Synthesis *via* cLIFT, derivatized with up to four glycan azides clicked to the peptide backbone. [8]

Figure 18. Fluorescence staining intensities of six different sugar-azide microarrays with ConA. We observe significant spacing-, density-, and ligand-dependent binding effects. [9]

These results have been published in:

[8] M. Mende, V. Bordoni, A. Tsouka, **F.F. Loeffler**, M. Delbianco, P.H. Seeberger, Multivalent glycan arrays, *Faraday Discuss.*, **2019**, 219, 9

[9] M. Mende, A. Tsouka, J. Heidepriem, G. Paris, D.S. Mattes, S. Eickelmann, V. Bordoni, R. Wawrzinek, F.F.

Building on these results, we made further progress in our in-situ generation of multivalent glycopeptides in the microarray format. We expanded our technology, making it compatible with different commercially available microarray surfaces, to probe previously inaccessible glycan interactions. Therefore, we first optimized the synthesis on different microarray surface types and we equipped them with an additional linker to investigate its effect on lectin binding. These optimizations improved the signal-to-noise ratios for our model lectin ConA by one order of magnitude, and helped to expand the applications for our synthesis platform to include weakly binding lectins. We could demonstrate the importance of surface accessibility and wettability on glycan-GBP interactions, enabling us to study a much wider range of plant lectins in a high-throughput manner. With these glycopeptide microarrays, we observed that the binding of lectins to different ligands strongly depends on glycan spacing, glycan density, microarray surface functionalization, and lectin concentration.

We have used this technology and synthesized other azido-sugars (Man, Glc, Gal, GlcNAc, GalNAc), which we clicked into the backbone and analyze additional multivalent interactions of several different lectins (WGA, PNA, SBA, RCA-1, DBA) and many different functional surfaces (Figure 19).

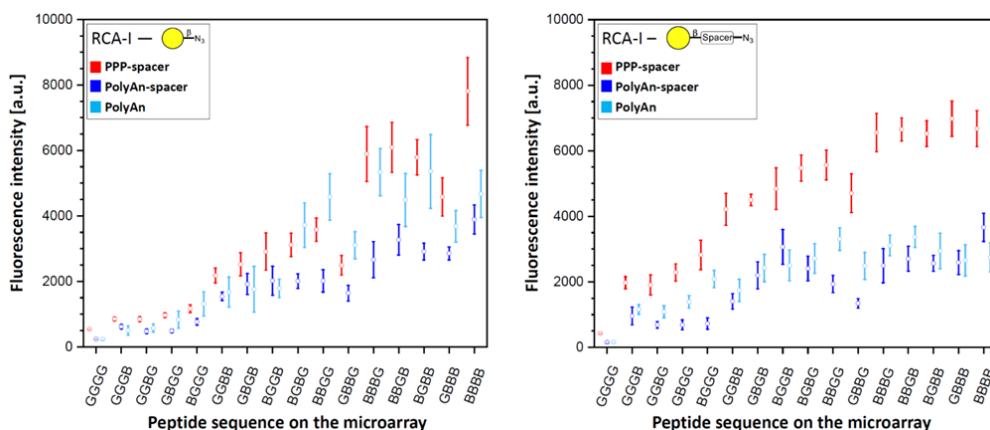


Figure 19. Example fluorescence staining intensities of (left) β -Gal azide 4 with RCA-I and (right) β -Gal-PEG3 azide 5 with RCA-I on PEPperPRINT slides with PEG-spacer (PPP-spacer; red), and on PolyAn functionalized slides with (dark blue) and without PEG-spacer (light blue). [10]

These results were published in:

[10] A. Tsouka, K. Hoetzel, M. Mende, J. Heidepriem, G. Paris, S. Eickelmann, P.H. Seeberger, B. Lepenies, **F.F. Loeffler**. Probing multivalent carbohydrate-protein interactions with on-chip synthesized glycopeptides using different functionalized surfaces. *Frontiers in Chemistry*, **2021**, 9, 766932

In addition, we have used this technology to explore them as potential encryption devices. Multichannel fluorescent devices can provide secure encryption by separately storing encrypted information in orthogonal fluorescent channels. However, current works typically require multiple fluorophores with different chemical structures or functional groups to obtain separable fluorescence channels,

which makes it easier to break the encryption. In our approach, we synthesized two positional isomers of 2,3-diphenylquinoxaline with an alkyne linker, enabling its immobilization on our array platform, this time using a carboxyl-azide building block for surface patterning/pre-functionalization. The alkyne linker donates electrons to the fully conjugated fluorophore system, which influences the electron shifting,

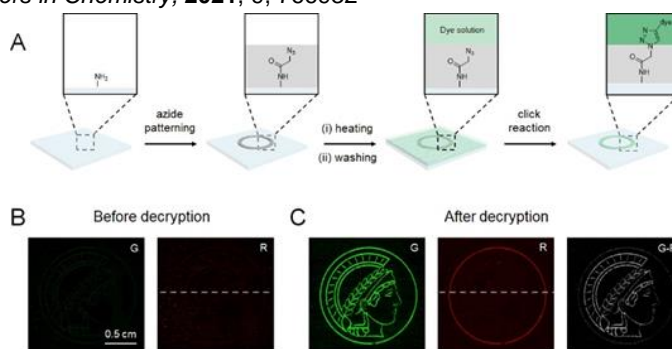


Figure 20. Multichannel fluorescent devices for encryption. (A) Schematic illustration of the construction of chemically-bound fluorescent patterns. Fluorescence image of an image pattern before (B) and after decryption (C).

especially after protonation. This further leads to asymmetric electron distribution and diametrically opposed change of intramolecular charge transfer processes, thereby emitting a shifted fluorescence in a different spectral range (Fig. 20), which can be confirmed by both experimental results and theoretical calculation. This work was a joint work with Prof. Merbouh (Simon Fraser University, Vancouver, Canada). This work was published:

[11] Y. Liu, P.H. Seeberger, N. Merbouh, **F.F. Loeffler**. Position Matters: Fluorescent Positional Isomers for Reversible Multichannel Encryption Devices. *Chemistry – A European Journal*, **2021**, 27, 16098–16102

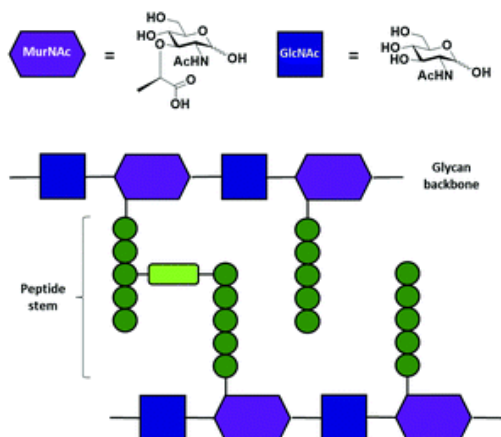


Figure 21. (top) Representation and structures of the two amino sugars, N-acetylglucosamine (GlcNAc) and N-acetylmuramic acid (MurNAc). (bottom) Schematic representation of the peptidoglycan structure. The different glycan strands are branched on the MurNAc residues with a sequence of amino acids (dark green circles) called stem peptide. An interpeptide bridge (light green box) may connect the two stem peptides. [12]

Finally, derived from these works with artificial glycopeptides, we have started a collaboration with Prof. Jon Laman (University Medical Center Groningen), regarding peptidoglycans (PGNs). These PGNs are integral parts of the bacterial cell wall (Fig. 21) of many pathogenic bacteria (e.g., *Staphylococcus aureus*) and are suspected to play a role in several inflammatory autoimmune diseases.

In a proof-of-concept, we have successfully synthesized ten different glycan fragments of the peptidoglycan backbone, using the automated glycan assembly synthesizer in our department.

This work was published in:

[12] P. Dallabernardina, V. Benazzi, J.D. Laman, P.H. Seeberger, **F.F. Loeffler**. Automated Glycan Assembly of Peptidoglycan Backbone Fragments. *Organic & Biomolecular Chemistry*, **2021**, 19, 9829–9832

Based on this work, we have established a stronger collaboration with Prof. Laman and have acquired joint funding to develop our platform for the synthesis of peptidoglycan microarrays, funded by the Dutch Research Council (NWO). This project offers large possibilities, especially in glycopeptide synthesis and autoimmune disease research.

WP 4 Generation and application of high-density microarrays

In WP 4, the main goal was to use the cLIFT technology for application in biomedical research, specifically for Flaviviruses (WP 4.1), malaria (WP 4.2), and autoimmune diseases (WP 4.3).

C. *difficile* screening of neutralizing antibodies

In a first collaboration with Prof. Michael Hust from the Technical University of Braunschweig, we first investigated their 31 newly generated antibodies towards their specificity to the toxin B of the superbug *C. difficile* (Fig. 22). We used the peptide array platform of Pepperprint. Together with the TU Braunschweig, we applied for a patent for the newly found neutralizing antibodies and the results were published:



Figure 22. Overview of epitopes mapped to TcdB in this study. Neutralizing epitopes are highlighted in red. Neutralizing epitopes published by others are designated in gray. [13]

investigated their 31 newly generated antibodies towards their specificity to the toxin B of the superbug *C. difficile* (Fig. 22). We used the peptide array platform of Pepperprint. Together with the TU Braunschweig, we applied for a

[13] V. Fühner, P. Heine, S. Helmsing, S. Goy, J. Heidepriem, **F.F. Loeffler**, S. Dübel, R. Gerhard, M. Hust. Development of neutralizing and non-neutralizing antibodies targeting TcdB of *Clostridium difficile*. *Frontiers in Microbiology*, **2018**, 9, 2908

Flavivirus screening (WP 4.1)

For a Flavivirus application, we focused on the Zika virus in a collaboration with Prof. Thomas Jänisch

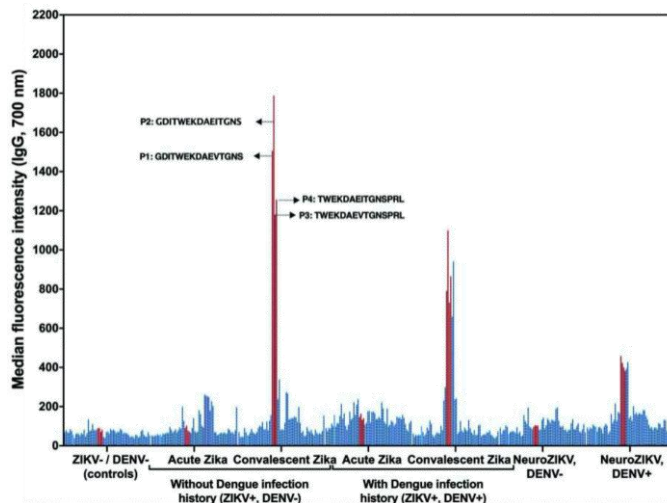


Figure 23. Identification of putative ZIKV NS2B epitopes. Immunoreactivity of the ZIKV NS2B peptides was individually assessed against the serum samples groups. Bars represent the median fluorescence intensity for individual peptides. Four peptides showing the highest fluorescence signals from the array are highlighted. [14]

(UC Denver), Dr. Roberto D. Lins, and Prof. Ernesto T.A. Marques (both Oswaldo Cruz Foundation, Recife, Brazil). The identification of specific biomarkers for Zika infection and its clinical complications is fundamental to mitigate the infection spread, which has been associated with a broad range of neurological sequelae. We characterized the antibody responses in serum samples from individuals infected with Zika, presenting non-severe (classical) and severe (neurological disease) phenotypes, with high-density peptide arrays from Pepperprint, comprising the Zika NS1 and NS2B proteins. The data pinpoints one strongly IgG-targeted NS2B epitope in non-severe infections (Fig. 23), which is absent in Zika patients, where infection progressed to the severe

phenotype. This differential IgG profile between the studied groups was confirmed by multivariate data analysis. Molecular dynamics simulations and circular dichroism have shown that the peptide in solution presents itself in a sub-optimal conformation for antibody recognition, which led us to computationally engineer an artificial protein able to stabilize the NS2B epitope structure. The engineered protein was used to interrogate paired samples from mothers and their babies presenting Zika-associated microcephaly and confirmed the absence of NS2B IgG response in those samples. These findings suggest that the assessment of antibody responses to the herein identified NS2B epitope is a strong candidate biomarker for the diagnosis and prognosis of Zika-associated neurological disease. A joint patent application was filed and the results were published:

[14] **F.F. Loeffler**, I.F.T. Viana, N. Fischer, D.F. Coêlho, C.S. Silva, C.M.C.S. Araújo, B.H.S. Leite, R. Durães-Carvalho, T. Magalhães, C.N.L. Morais, M.T. Cordeiro, R.D. Lins, E.T.A. Marques, T. Jaenisch. Identification of a Zika NS2B epitope as a biomarker for severe clinical phenotypes. *RSC Medicinal Chemistry*, **2021**, 12, 1525–1539

Malaria screening (WP 4.2)

Then, we used the high-throughput peptide array technology from Pepperprint for malaria research, analyzing patient sera from individuals living in malaria endemic regions in Africa (collaboration with Prof. Thomas Jänisch, UC Denver). The arrays enabled us to correlate between the clinical phenotype and the antibody response against linear epitopes of the *Plasmodium falciparum* proteome. Peptides from twelve known vaccine candidate proteins and a bioinformatical selection were screened. Strong reactivities to epitopes derived from known vaccine candidates as well as new immunogenic proteins were identified (Fig. 24). Peptide arrays are a versatile tool for the analysis and correlation of antibody response profiles, associated with pathology or protection. This screening and the results may serve well as a database, to address a wide range of scientific questions in malaria vaccine and biomarker development.

The results were published in:

[15] T. Jaenisch, K. Heiss, N. Fischer, C. Geiger, F. R. Bischoff, G. Moldenhauer, L. Rychlewski, A. Sié, B. Coulibaly, P.H. Seeberger, L.S. Wyrwicz, F. Breitling, **F.F. Loeffler***. High-density peptide arrays help to identify linear immunogenic B cell epitopes in individuals naturally exposed to malaria infection. *Molecular & Cellular Proteomics*, **2019**, 18, 642–656

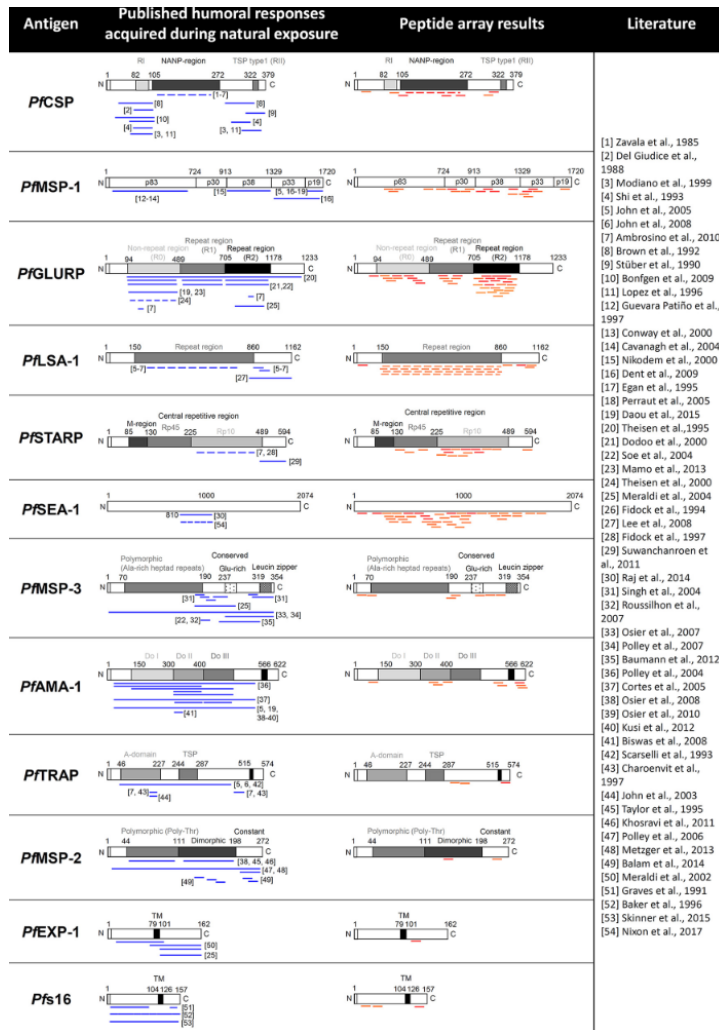


Figure 24. Comparison of vaccine candidate peptide array results with selected literature references. Immunogenic linear peptide epitopes selected from literature (blue) and identified in the peptide array approach (orange: p-value < 0.05, red: p-value < 0.01) with 12 vaccine candidates. [15]

Ebola antibody screening

In a collaboration with Prof. Stephan Becker from the University in Marburg and Prof. Marylyn Addo from the University Hospital in Hamburg, we investigated the immune response to the Ebola virus. The Ebola virus (EBOV) can cause severe infections in humans, leading to a fatal outcome in a high percentage of cases. Neutralizing antibodies against the EBOV surface glycoprotein (GP) can prevent infections, demonstrating a straightforward way for an efficient vaccination strategy. Meanwhile, many different anti-EBOV antibodies have been identified, whereas the exact binding epitopes are often unknown. We presented the analysis of serum samples from an EBOV vaccine trial with the viral vector vaccine rVSV-ZEBOV and an Ebola virus disease survivor, using

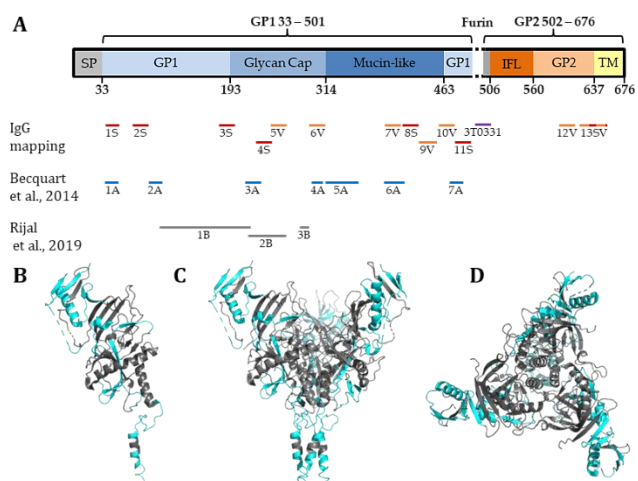


Figure 25. Epitopes of the EBOV glycoprotein. **A**) Comparison of the immunogenic epitopes of the EBOV GP. The found IgG epitopes in the survivor (S) and vaccinees (V) compared to epitopes published in the literature. **B–D**) 3D view of the EBOV GP structure with the identified IgG epitopes (vaccinees and survivor) highlighted in cyan. **B**) Side view of GP monomer **C**) side view of GP trimer. **D**) Top view of GP trimer. [16]

high-density peptide arrays. In this proof-of-principle study, we detected distinct IgG and IgM antibodies binding to different epitopes of EBOV GP: By mapping the whole GP as overlapping peptide fragments, we found new epitopes and confirmed epitopes from the literature (Fig. 25). Furthermore, we could validate the highly selective binding epitope of a neutralizing monoclonal anti-EBOV GP antibody. This shows that peptide arrays can be a valuable tool to study the humoral immune response to vaccines in patients and to support Ebola vaccine development, published in:

[16] J. Heidepriem, V. Krähling, C. Dahlke, T. Wolf, F. Klein, M.M. Addo, S. Becker, **F.F. Loeffler**. Epitopes of naturally acquired and vaccine-induced anti-Ebola virus glycoprotein antibodies in single amino acid resolution. *Biotechnol. J.*, **2020**, 15, 2000069

Proof-of-principle cLIFT synthesis of Ebola proteome

While we initially planned to synthesize arrays for application in Flavivirus and malaria research (WP 4.1 & 4.2) using cLIFT, we used the already available Peppereprint technology due to time restrictions. Since we have already use the Pepperprint technology for Flavivirus screenings, to achieve the central milestone M3 in WP 4, i.e. the cLIFT generation of Flavivirus arrays for screening of Flavivirus patients, we shifted the synthesis application to the Ebola proteome [1]. Using and finally validating our cLIFT approach, we synthesized 1600, 4444, and 10000 spots/cm² peptide microarrays containing the Ebola virus surface glycoprotein and analyzed the IgG response of an Ebola virus disease survivor (Fig. 26). The results showed a high reproducibility with robust epitope detection, independent of the spot density. Compared to a commercial reference Ebola virus surface glycoprotein microarray, we not only identified the same epitopes with improved signal to noise ratio, but also detected additional epitopes that are known from literature using ELISA peptide screening platforms. These results imply that we achieve high quality syntheses. High density peptide microarrays (4444 and 10000 spots/cm²) containing the complete Ebola virus proteome for the first time in single amino acid resolution (4805 individual peptides) provide an excellent tool to study the IgG response of an Ebola virus infection survivor. The results were published in [1] (see WP 1).

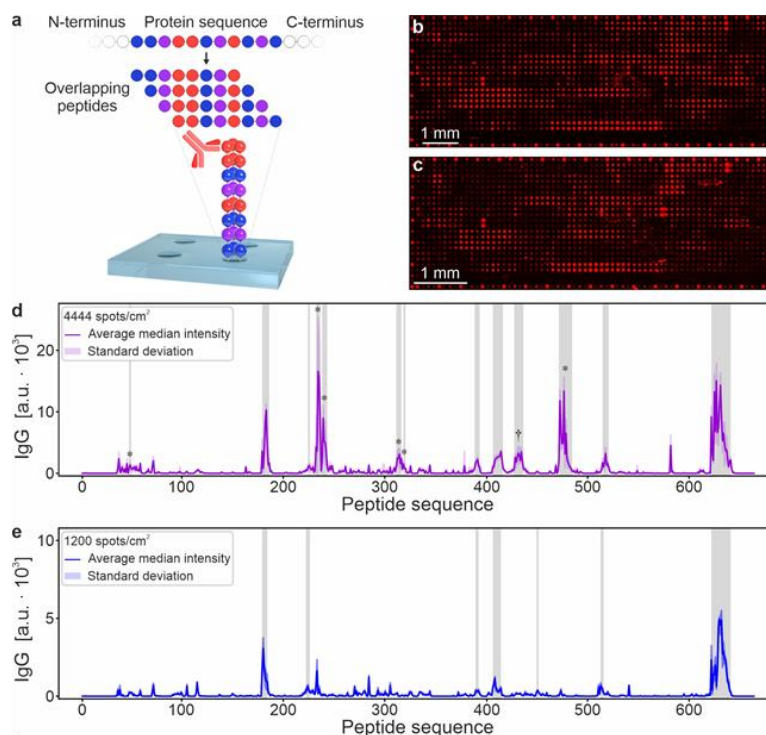


Figure 26. Synthesized Ebola virus surface glycoprotein peptide microarrays for IgG antibody screening of a disease survivor. (a) The Ebola virus surface glycoprotein sequence was mapped as 662 overlapping 15 residue peptides with a lateral shift of one AA (as spot duplicates). (b, c) After serum incubation, antibody binding to arrays with (b) 4444 and (c) 10000 spots/cm² was analyzed with fluorescence imaging and data presented as mean (of median IgG value) ± SD. (d) The resulting signals of the 4444 spots/cm² (n = 10, background subtraction of 400 a. u.) and (e) commercial reference microarrays (n = 8, background subtraction of 162 a. u.) are shown. Our synthesized microarray was able to detect more epitopes than the commercial array. Epitopes are highlighted in grey (*: known from literature; †: newly identified) [1].

In addition, we have used Pepperprint peptide microarrays to screen SARS-CoV2 patients for their serum antibody response and a MERS Corona vaccine recipients, in collaboration with our partners from Hamburg (Prof. Addo):

- [17] J. Heidepriem, C. Dahlke, R. Kobbe, R. Santer, T. Koch, A. Fathi, B.M.S. Seco, M.L. Ly, S. Schmiedel, D. Schwinge, S. Serna, K. Sellrie, N.-C. Reichardt, ID-UKE COVID-19 study group, P.H. Seeberger, M.M. Addo, **F.F. Loeffler**. Longitudinal development of antibody responses in COVID-19 patients of different severity with ELISA, peptide, and glycan arrays: an immunological case series. *Pathogens*, **2021**, 10, 438
- [18] A. Fathi, C. Dahlke, A. Kupke, V. Krähling, N. M. A. Okba, M. Raadsen, J. Heidepriem, G. Paris, M. Müller, S. Lassen, M. Kluever, S. Halwe, C. Rohde, M. Eickmann, A. Volz, T. Koch, M. L. Ly, M. Friedrich, R. Fux, A. Tscherne, G. Kalodimou, S. Schmiedel, A. W. Lohse, V. Corman, T. Hestekamp, C. Drosten, **F.F. Loeffler**, B. L. Haagmans, G. Sutter, S. Becker, M.M. Addo. Increased neutralization and IgG epitope identification after MVA-MERS-S booster vaccination against Middle East respiratory syndrome. *Nature Communications*, **2022**, 13, 4182

Autoimmune disease application (WP 4.3)

For applications in autoimmune disease (WP 4.3), we focused on peptidoglycans in the collaboration with Prof. Laman (Uni Groningen, see WP 3). The project is still ongoing and requires more time, since the cLIFT platform needs to be adapted to the synthesis of the much more complex peptidoglycans. The postdoctoral researcher, who was in charge of the project had unfortunately left for an industry position, which significantly delayed the project.

WP 5 Matrix-based combinatorial synthesis

In WP 5, the cLIFT process should be optimized with a chemical vapor approach (WP 5.1) to enable other chemical reactions with the platform. In addition, the cLIFT synthesis of peptoids (WP 5.2) and oligosaccharides should be explored (WP 5.3).

Peptoid synthesis (WP 5.2)

In collaboration with the group of Prof. Frank Breitling, Dr. Daniela Mattes, and Prof. Stefan Bräse from the Karlsruhe Institute of Technology, together with Prof. Bernhard Spengler from the University of Giessen, we have developed a process, where we can synthesize peptoids with the cLIFT process and subsequently, we were able to validate the synthesis via MALDI imaging, directly on the surface. We generated peptoid arrays with a density of 10 000 spots/cm² with the sub-monomer or monomer peptoid synthesis method. In Figure 27, the peptoid synthesis cycle for submonomer method is shown. The important step is the transfer of an amine derivative, which is transferred with the laser, followed by a coupling reaction in the polymer matrix material, exploiting a nucleophilic substitution reaction. Thus, we could show that the cLIFT method is also compatible with other (but yet similar)

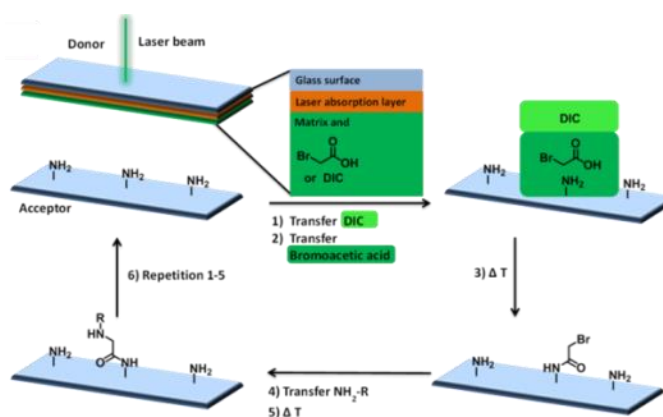


Figure 27. Synthesis of peptoid arrays with the submonomer method via cLIFT: 1, 2) DIC and bromoacetic acid are transferred to the surface (alternatively an active ester of bromoacetic acid). 3) Coupling in the oven. 4) Amine transfer. 5) Coupling in the oven or via solvent vapor. 6) Repetition 1-5. [19]

chemical syntheses.

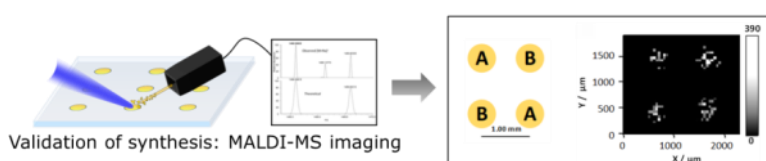


Figure 28. MALDI imaging analysis of the synthesized peptoids. Lateral resolution was set to 50 μm/pixel.

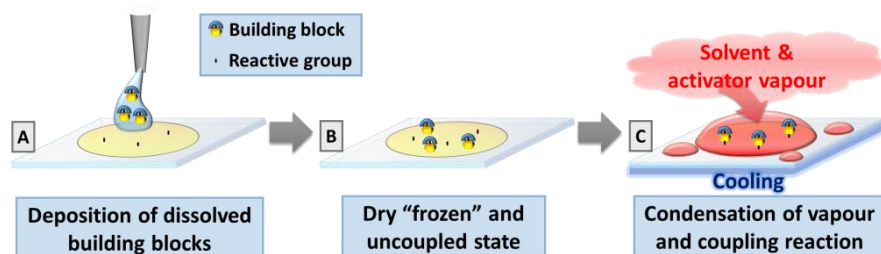
Furthermore, for the first time, we verified successful reactions spot-by-spot, by laser-transferring MALDI-matrix, followed by MALDI mass spectrometry imaging (Fig. 28).

This is the first result, showing the validation of a synthesis in an imaging approach. The results were published in:

[19] D.S. Mattes, B. Streit, D.R. Bhandari, J. Greifenstein, T.C. Foertsch, S. Muench, B. Ridder, C.v. Bojničić-Kninski, A. Nesterov-Mueller, B. Spengler, U. Schepers, S. Bräse, **F.F. Loeffler***, F. Breitling*. Synthesis of peptoid arrays via matrix-based combinatorial laser transfer. *Macromolecular Rapid Communications*, **2018**, 40, 1800533

Chemical vapor and oligosaccharide synthesis (WP 5.1 & 5.3)

Currently, there is no parallelized chemical synthesis method for carbohydrates available. Therefore, we



we have developed a novel concept to separate the patterning of chemical building blocks, such as saccharide building blocks, from the actual chemical (glycosylation) reaction step (Fig. 29).

Figure 29. Concept of VaporSPOT.

First, the building block is dissolved (or embedded in a polymer) and deposited onto a substrate (cellulose membrane or functionalized glass surface). The solvent dries/evaporates, while no reaction occurs, because the activating reagent is missing. Then, the substrate is brought into a dry and cooled chamber. Finally, a vapor of solvent and activator is injected, condensing on the substrate and driving the reaction. This step allows for a chemical reaction at low temperatures, whereas the precision of the deposition pattern can be preserved. Since we combine this vapor approach with the SPOT synthesis (spotting of compounds in a solvent onto a membrane), we call this principle VaporSPOT (patent filed 2018).

VaporSPOT enables the simultaneous synthesis of different oligosaccharides on a cellulose membrane solid support. Different linkers allow for flexible and straightforward cleavage, purification, and characterization of the target oligosaccharides. This method is the basis for the development of parallel automated glycan synthesis platforms and was published in:

[20] A. Tsouka, P. Dallabernardina, M. Mende, E.T. Sletten, S. Lechnitz, K. Bienert, K.L.M. Hoang, P.H. Seeberger, **F.F. Loeffler***. VaporSPOT: Parallel synthesis of oligosaccharides on membranes. *Journal of the American Chemical Society*, **2022**, 144, 19832–19837

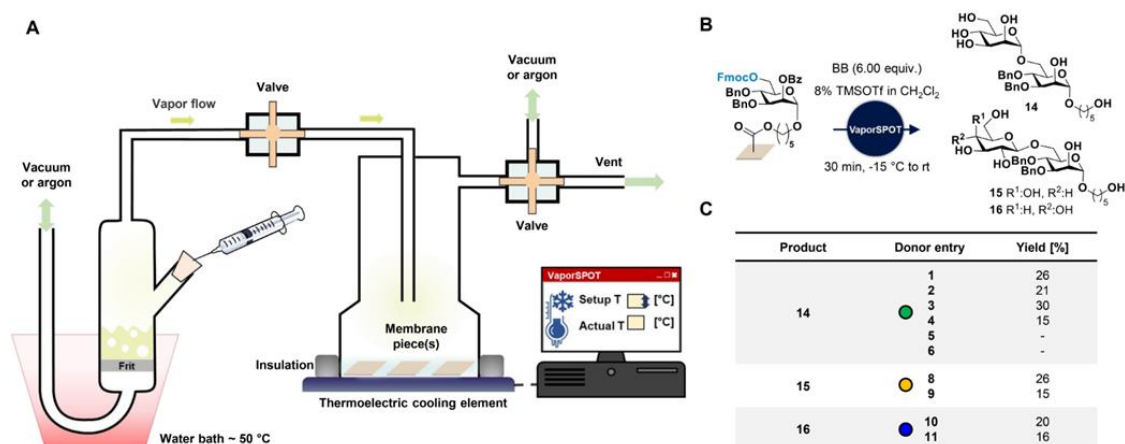


Fig. 30. (A) Schematic representation of the custom-built apparatus for parallel and temperature controlled VaporSPOT oligosaccharide synthesis on membranes. (B) Screening of BBs 1-6 and 8-11 under the same vapor glycosylation conditions (8% TMSOTf in dichloromethane) for the synthesis of dimers 14-16. (C) Obtained yields after cleavage and characterization of the target dimers. [20]

Derived from this VaporSPOT approach, we developed the VaporLIFT method for parallel in situ chemical synthesis of glycan microarrays (Fig. 31). It integrates the high-throughput capabilities of laser-induced forward transfer (LIFT) with the vapor synthesis method (VaporSPOT) to facilitate the parallelization of chemically demanding reactions, such as glycosylation. While LIFT is effective for generating precise spot patterns containing matrix-embedded chemical building blocks (BBs) on a solid

support, it is typically limited to robust reactions like amide bond formation, since the coupling reaction relies on heat induction in an oven (95 °C). On the other hand, VaporSPOT excels in enabling parallel temperature- and moisture-sensitive glycosylation reactions but is restricted by lower throughput and manual spotting requirements. VaporLIFT overcomes these limitations by combining the strengths of both LIFT and vapor synthesis. This method allows for the rapid generation of glycans on microarray surfaces under inert, low-temperature conditions necessary for glycosylations. Chemical building blocks embedded in a polymer matrix are transferred and coupled in defined patterns on a surface, and subsequent parallel activation and glycosylation occur in a specially designed controlled chamber with activator vapor. This process was optimized for the synthesis of diverse glycans at specific locations on a glass surface, with the synthetic structures detected by mass spectrometry, fluorescently labeled glycan-binding proteins, and covalent staining with fluorescent dyes. VaporLIFT is particularly well-suited for the parallel screening of other chemical reactions that require precise and inert reaction conditions. This was published in:

[21] A. Tsouka, M. Mende, J. Heidepriem, P. Dallabernardina, K. Bienert, P.H. Seeberger, **F.F. Loeffler***. VaporLIFT: On-chip chemical synthesis of glycan microarrays. *Advanced Functional Materials*, **2024**, 2310980

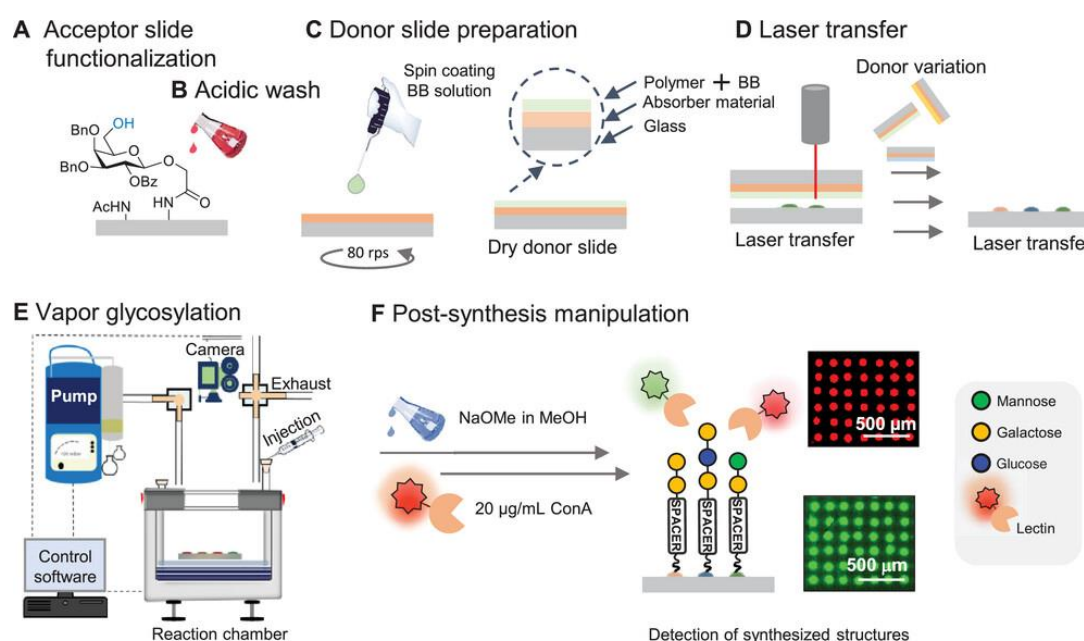


Figure 31. Schematic representation of the VaporLIFT process. (A) Functionalization of acceptor glass slide; (B) Acidic wash of the functionalized acceptor; (C) Preparation of glycosyl donor slides via spin coating. BB: building block. (D) Transfer of the glycan BB in polymer matrix by LIFT. (E) Computer-controlled vapor glycosylation setup with vacuum pump, cooled reaction chamber, camera, injection and exhaust valve. (F) Post-synthesis manipulation; deprotection and validation with fluorescently labeled lectins. [21]

Furthermore, we have shown the proof-of-concept that we can perform also other chemical reactions in our polymer directly on surfaces, such as click chemistry [5]. Furthermore, we show that condensation reactions (Schiff base reaction, Fig. 32a) are possible with sequential cLIFT synthesis, forming fluorescent aromatic donor/acceptor molecules in a defined pattern on the solid phase substrate (Fig. 32b). Thus, we have successfully achieved the central milestone **M4** of WP 5.2, producing a non-peptidic organic molecule via cLIFT. In addition, we have also explored the potential of the platform for high-throughput reaction screening: We patterned two different dyes, embedded in polymer donor slides, mixing/stacking the two dyes in different concentrations via tuning the laser energy (Figure 32c,d) [1]. This is useful to perform pre-mixing of reaction partners directly on a surface, where each spot is its individual reactor. These results show the large potential of the technology to perform high-throughput reaction screenings on a surface in parallel.

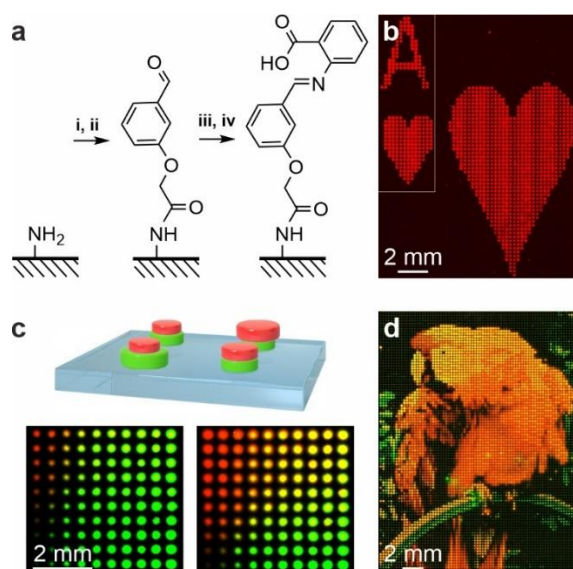


Figure 32. Laser-based synthesis of fluorophore arrays. (a) (i, ii) Activated 2-(3-formylphenoxy)acetic acid was transferred and coupled to the surface via amide bond formation. (iii, iv) 2-aminobenzoic acid was transferred and reacted, forming the Schiff base 2-((3-(carboxymethoxy)benzylidene)amino)benzoic acid. (b) Fluorescence image of the synthesized Schiff base microarray. (c) Experimental screening of laser transfer parameters for two fluorescent dyes in a polystyrene co-polymer (green: Rhodamine 6G, red: Nile blue A) to obtain a precise red green color mixing (resulting in yellow). (d) Optimal parameters enable the production of a 75 x 100 pixel (i.e., spot) image with thousands of different color ratios. [1]

Additional findings

Derived from the laser-induced forward transfer (LIFT) principle, we have developed a novel technology, which we call laser-driven transfer synthesis (LTRAS, Fig. 33). In this approach, we show for the first time that our continuous wave laser process can not only transfer but, at the same time, also drive a chemical reaction to generate precisely controlled composite materials *in-situ* on different surfaces (e.g., glass, fluorine-doped tin oxide (FTO), carbon, carbon nitride (CN)). In the laser system, the configuration of the composite film can be flexibly tuned by laser parameters: pattern (location), shape and assembly size, and the sequence of different materials (e.g., sequential deposition of different precursor materials). We use the LTRAS method to generate CuO/CN composite films as photoanodes. Thin-layer CuO nanostructures with controllable size and shape are obtained on the CN substrate. Nano-structured p-n junctions are created due to the spatial organization of the composite layers. The CuO morphology significantly influences charge transport and distributions in the films that further changes the efficiency of photogenerated charge separation and transfer. These as-prepared electrodes can be applied as highly efficient photoelectrochemical glucose sensors. In the future, this approach may significantly shorten the synthesis time for the direct synthesis of peptides on arrays without the oven coupling step.

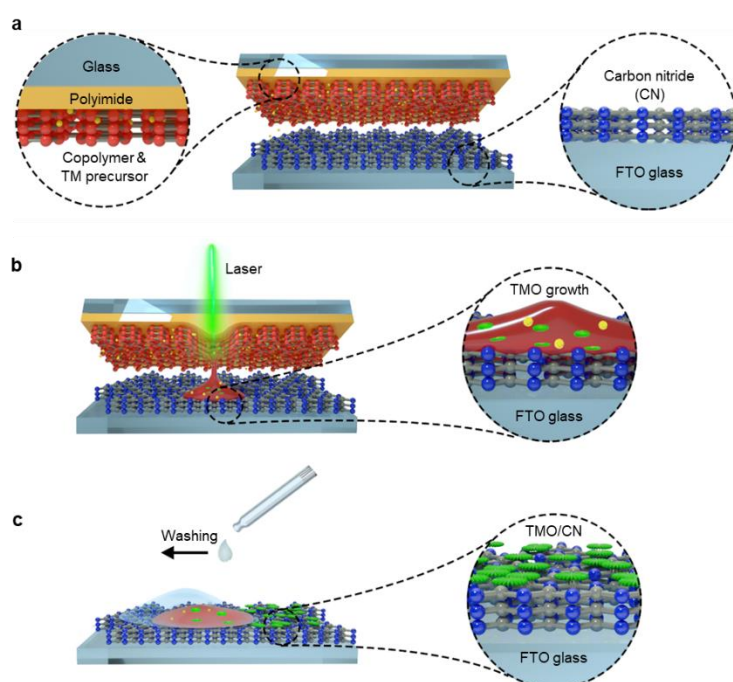


Figure 33. Principle of the laser-driven transfer synthesis (LTRAS) process for the generation of single-layer transition metal oxide/carbon nitride (TMO/CN) composite films. (a) Laser irradiation transfers material from a donor to an acceptor surface. The donor slide is prepared by spin coating a mixture of dissolved copolymer together with transition metal (TM) precursor onto a polyimide-coated glass slide. The acceptor slide is prepared by vapor deposition polymerization of CN onto an FTO glass slide. (b) The laser rapidly heats, melts, and transfers the donor material. At the same time, the decomposition temperature of the metal precursor is reached and TMO structures are formed. (c) After a short rinsing with acetone, the TMO/CN composite film is ready. [22]

The process has been published in:

[22] J. Zhang, Y. Zou, T. Heil, C. Njel, S. Eickelmann, S. Ronneberger, V. Strauss, P.H. Seeberger, A. Savateev, **F.F. Loeffler**. Laser-driven growth of structurally defined transition metal oxide nanocrystals on carbon nitride photoelectrodes in milliseconds. *Nature Communications*, **2021**, 12, 3224

In addition, we have further developed this laser-driven transfer and synthesis approach (LTRAS) for the synthesis of carbon nanodots with an application in anti-counterfeiting. Besides causing trillion-dollar economic losses every year, counterfeiting (i.e., fake products) threatens human health, social equity, and national security. Current materials for anti-counterfeiting labeling typically contain toxic inorganic quantum dots and the techniques to produce unclonable patterns require tedious fabrication or complex readout methods. Here, we developed a nanoprinting-assisted flash synthesis approach, which generates fluorescent nanofilms with physical unclonable function (PUF) micropatterns in milliseconds. This flash synthesis approach yields quenching-resistant fluorescent carbon nanodots in solid films, directly synthesized via LTRAS from simple monosaccharides, such as glucose (Fig. 34). Since the laser technology allows for high-throughput synthesis, we quickly established a nanofilm library comprising 1,920 experiments, offering conditions for various optical properties and microstructures. We produce 100 individual PUF patterns exhibiting near-ideal randomness (bit uniformity 0.492 ± 0.018), high uniqueness (0.498 ± 0.021), and reliability ($> 93\%$) that is ideal for anti-counterfeiting applications. These unclonable patterns can be quickly and independently read out by fluorescence and topography scanning, highly improving their security.

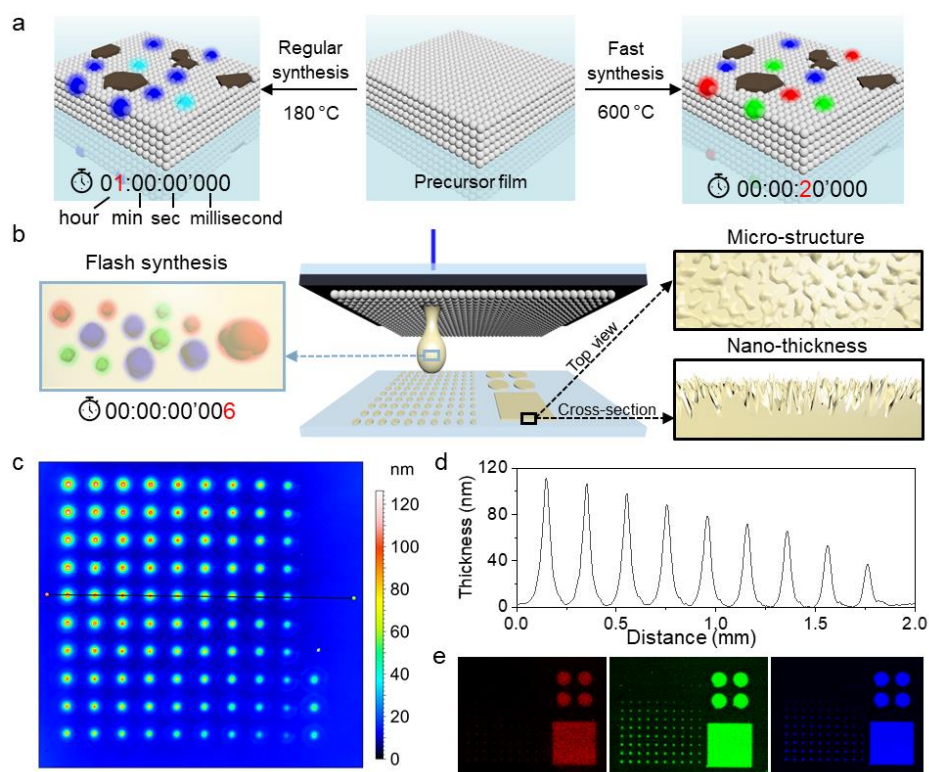


Figure 34. Principle of nanoprinting-assisted flash synthesis approach and characterization of transferred patterns. (a) Solvent-free synthesis of fluorescent carbon dots from glucosamine in an air oven. (b) Fluorescent patterns with microstructures were generated by laser-driven transfer of precursors. Height map (c) and profile (d) of a transferred spot gradient show material height in nanoscale. (e) Fluorescence scanning using 635, 532, and 488 nm excitation channels. For the square area, the bitmap mode was used with 105 mW laser power and 100 mm s⁻¹ scanning speed. The gradient began at the right bottom corner (12 mW laser power, 1 ms). The laser power increased by 13 mW per line and the irradiation time increased by 1 ms per row.

This synthesis method is an all-in-one strategy to *in-situ* generate solid state fluorescent carbon nanodot films and simultaneously print unclonable nano-/micro-structures. During the normal solvent-free synthesis in an oven, large carbon flakes, formed by over-carbonization, cause fluorescence quenching. Our approach avoids this problem by precisely controlling the heating process in milliseconds. The

generated carbon dots are dispersed in the non-reacted monosaccharide precursor, which highly reduces Förster resonance energy transfer, whereas typical carbon nanodots do not fluoresce in solid state due to quenching. Therefore, the carbon dot nanofilms show quenching-resistant properties. We generated a nanofilm library of 1,920 experimental datasets with tunable fluorescence from violet-blue to red and different microstructures. The distinct randomness of the microstructures allows the nanofilms to be used as PUF patterns (Fig. 35). Near-ideal bit uniformity, high uniqueness, and reliability were observed, suggesting their excellent PUF performance. Furthermore, the combination of independent fluorescence and topography readout highly improves the security level of the PUF patterns (Fig. 35), making them immune to attacks by nanomolding and nanolithography. Through an open-source deep learning algorithm, a significant gap between the intra- and intercorrelation promises precise authentication regardless of the readout methods (fluorescence or white light interferometry) the end users choose. Concluding, our technique solves the challenges in the *in-situ* synthesis of carbon nanodots with solid state fluorescence and offers unique micropatterns with excellent PUF properties. The fluorescent film library provides efficient guidance for future syntheses, or practical applications, such as color conversion layers, quenching-resistant (O)LEDs, or sensitive bio-/chemosensors. It will also expand the scope of the cLIFT approach for future high-throughput syntheses of biomolecules.

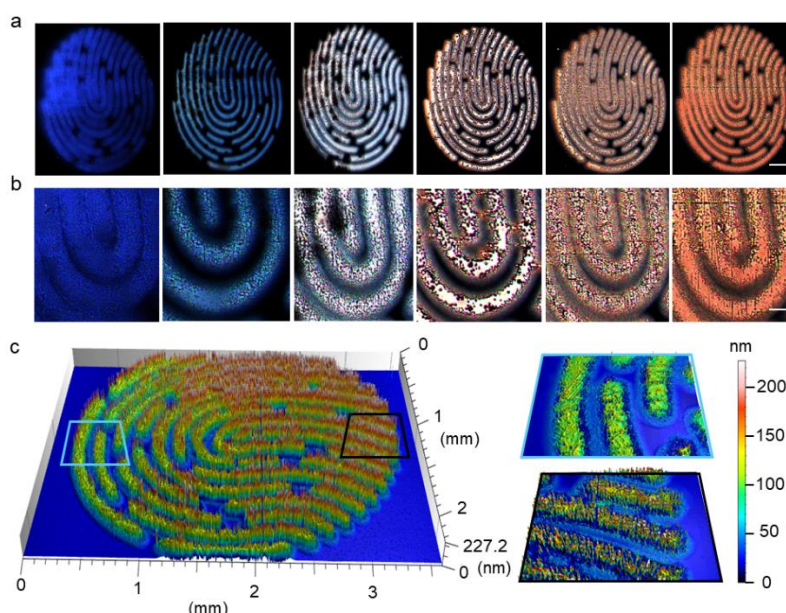


Figure 35. Artificial fingerprints with micro-morphology and nano-thickness. (a) Fingerprint patterns with different fluorescent colors were generated based on the library. Scale bar: 500 μm . (b) Magnification showing the micro-morphology of the patterns. Scale bar: 100 μm . (c) 3D height map of fingerprint pattern (right figure in (a)). [23]

These results have been published in a high impact journal:

[23] J. Zhang, Y. Liu, C. Njel, S. Ronneberger, N. V. Tarakina, **F.F. Loeffler***. An all-in-one nanoprinting approach for the synthesis of a nanofilm library for unclonable anticounterfeiting applications. *Nature Nanotechnology*, **2023**, 18, 1027–1035

Conclusion

The above results show that all major milestones have been successfully reached. While the cLIFT approach has been successfully adapted by the company Pepperprint (project partner), further research and development have to be performed to transfer the oligosaccharide approach to an industrial application (VaporSPOT & VaporLIFT). Great future perspectives have been opened with the laser transfer and synthesis approach, which may speed up chemical synthesis for high-throughput applications and screenings.

2. Wichtigste Positionen des zahlenmäßigen Nachweises

Der größte Posten waren mit 1.731.752,19 € Personalausgaben für den Gruppenleiter, fünf Doktorand:innen, drei 3 Postdocs und mehrere studentische Hilfskräfte, die für die Durchführung der FuEul-Arbeiten essenziell waren. Weitere große Positionen betrafen Verbrauchsmaterialien mit 327.255,49 € (insbesondere Chemikalien, Lösungsmittel, Antikörper, funktionalisierte Oberflächen, sowie eine Overheadpauschale i.H.v. 10% auf Personalausgaben), Dienstreisen mit 20.446,82 € (insbesondere Konferenzreisen, Einladung von Gastwissenschaftler:innen und Forschungsaufenthalte) und die Anschaffung von Geräten für Forschungszwecke mit 180.343,84 € (insbesondere ein Weißlichtinterferometer zur nanometrischen Höhenprofilmessung und Komponenten für den Syntheseroboter wie z.B. Optiken und Laser). Alle getätigten Ausgaben waren für die Zielerreichung notwendig. Es wurde zu jeder Zeit sparsam gewirtschaftet.

3. Notwendigkeit und Angemessenheit der geleisteten Projektarbeiten

Mit diesem Projekt hat der Antragsteller eine unabhängige Nachwuchsgruppe mit eigenen Doktoranden und zusätzlichem wissenschaftlichem Personal erfolgreich am MPI für Kolloid- und Grenzflächenforschung etabliert. Für den Aufbau dieser Arbeitsgruppe wurden die beantragten Mittel verwendet, die vom Gastinstitut aufgrund des begrenzten institutionellen Budgets und dem relativen Risiko dieser anwendungsorientierten Forschung nicht aufgebracht werden konnten. Daher hätte das Projekt cLIFT ohne öffentliche Förderung nicht im beschriebenen Umfang durchgeführt werden können. Alle Ausgaben und Arbeiten dienten den Zielen des beantragten cLIFT Projekts, zur Weiterentwicklung der Laser-basierten Drucktechnologie und deren Anwendungen.

4. Voraussichtlicher Nutzen und Fortschreibung des Verwertungsplans

Die wissenschaftlich-technische und auch die wirtschaftliche Anschlussfähigkeit ergeben sich aus folgenden Punkten: (i) Mittels Peptidarrays konnten spezifische Antikörper für Infektionskrankheiten wie Ebola oder Zika bestimmt werden und daraus potentielle Biomarker entwickelt werden. Die Anwendung von Proteom-Peptidarrays kann nun für viele weitere Krankheiten etabliert werden. (ii) Für die Dampf-basierte parallele Herstellung von Arrays für andere organische Moleküle (z.B. Zuckerstrukturen oder Glykopeptidstrukturen) konnten wir ein Patent anmelden. Die Technologien für die Herstellung von Peptidarrays und Glykopeptidarrays sind für Firmen wie z.B. Pepperprint äußerst interessant. Für die weitere Entwicklung der Glykopeptidarrays sollen weitere Gelder eingeworben werden und es wird eine Ausgründung erwägt. Eine solche Ausgründung könnte im Wesentlichen auf die in diesem Projekt weiter entwickelte cLIFT-Synthesemaschine gründen, die nicht besonders teuer ist. Außerdem können die Weiterentwicklungen der LIFT Methode zur Lasertransfer und Synthese (LTRAS) neue Anwendungen in der Materialforschung und der Produktsicherheit ermöglichen. Des Weiteren wurden die erzielten F&E-Ergebnisse nach Patentierung in hochrangigen Journalen veröffentlicht, die die Grundlage für weitere Entwicklungen in der öffentlichen und privaten Forschung liefern.

5. Darstellung des während der Durchführung des Vorhabens dem Zuwendungsempfänger bekannt gewordenen Fortschritts auf dem Gebiet des Vorhabens bei anderen Stellen

Während der Dauer des Projekts sind dem Zuwendungsempfänger keine relevanten Fortschritte von anderen Forschungsinstituten oder Firmen auf dem Gebiet des Vorhabens bekannt geworden.

6. Erfolgte oder geplante Veröffentlichungen des Ergebnisses

Die zentralen Publikationen aus dem Projekt wurden im Bericht erwähnt. Die vollständige Liste aller mit dem Projekt verbundenen Veröffentlichungen wurde eingereicht.